ENGINEERING *SACCHAROMYCES CEREVISIAE* FOR CELLULOSIC ETHANOL PRODUCTION

BY

HAIQING XU

THESIS

Submitted in partial fulfillment of the requirements
for the degree of Master of Science in Food Science and Human Nutrition
with a concentration in Food Science
in the Graduate College of the
University of Illinois at Urbana-Champaign, 2015

Urbana, Illinois

Master's Committee:

Associate Professor Yong-Su Jin, Chair
Professor Timothy A. Garrow
Associate Professor Michael J. Miller

ABSTRACT

There are two long-existing obstacles for cellulosic ethanol production in *Saccharomyces cerevisiae*. The first one is inefficient xylose utilization and the second one is sequential fermentation of glucose and xylose in engineered *Saccharomyces cerevisiae*. This study mainly focused on solving these two problems by using cutting edge synthetic biology tools.

A phosphatase enzyme of unknown specificity in *Saccharomyces cerevisiae*, Pho13, plays a role in the transcriptional regulation of genes related to pentose phosphate pathway (PPP) and NADPH regeneration. It has been also reported that deletion of *PHO13* (*pho13Δ*) in *S. cerevisiae* results in significantly improved xylose metabolism in engineered strains metabolizing xylose. However, it has not been elucidated whether the transcriptional activation caused by *pho13Δ* is associated with the metabolic changes favoring xylose fermentation. We investigated the global metabolic changes in response to *pho13Δ* to understand underlying mechanisms of the enhanced xylose fermentation upon *pho13Δ*. Among the 134 metabolites identified in cells grown on xylose, the concentration of sedoheptulose decreased by 98% in the *pho13Δ* mutant as compared to that of a parental strain. Sedoheptulose is not a common metabolite but a dephosphorylated form of sedoheptulose-7-phosphate (S7P), was also significantly decreased by *pho13Δ*. As S7P is a substrate of transaldolase (*TAL1*) in PPP, we hypothesized that *TAL1* upregulation induced by *pho13Δ* might be responsible for the reduced accumulation of S7P and sedoheptulose, leading to improved xylose fermentation. We constructed various mutants overexpressing *TAL1*, and monitored their metabolic and phenotypic changes. Increased *TAL1* expression levels were correlated with reduced sedoheptulose levels, and increased xylose consumption rates. While other transcriptional and metabolic changes

induced by *pho13Δ* were identified, we concluded that *TAL1* upregulation that prevents sedoheptulose accumulation is the most important mechanism for improved xylose metabolism.

Because of the strong inhibition of glucose to xylose at the transport level, transporter engineering is believed to be the prerequisite for achieving co-fermentation of glucose and xylose in *Saccharomyces cerevisiae*. Platform strains with native major sugar transporters deletion and a robust xylose metabolism pathway are required for studying transporters for co-fermentation. However, previously reported transporters studies were greatly restricted by their platform strains, which either suffered from the gene loss and genome rearrangement during the serial transporters deletion or their ineffective xylose metabolism pathway. In this study, we applied the CRISPR/Cas9 guided multiple-gene deletion technique to refactor a fast xylose-fermenting *Saccharomyces cerevisiae* strain to a sugar-transport-deficient platform strain. With this platform strain, we investigated the xylose and glucose fermentation capacities of two mutant Gal2 transporters, Gal2-N376F and Gal2-N376V, and fulfilled their potentials of co-fermentation of glucose and xylose. By the combination of two mutant Gal2 transporters, we constructed a co-fermenting mutant, which could ferment mixture of glucose and xylose as fast as the original sequential-fermenting strain. Moreover, we also set up the first *Saccharomyces cerevisiae* co-culture system to co-ferment glucose and xylose by using two yeast strains with opposite substrate selectivity. These studies demonstrated the efficiency of the CRISPR/Cas9 based multiple-gene deletion technique and the feasibility of transporters engineering to enable co-fermentation of glucose and xylose in industrially relevant concentrations without compromising the fermentation rate and the ethanol yield.

ACKNOWLEDGEMENTS

I would like to thank my advisor Dr. Yong-Su Jin, who endowed me with the great opportunity to join his lab to do research and provided me with endless help and instruction during my master's study. His curiosity and motivation towards science inspire me to pursue a long-term career in science. Most importantly, he builds up a lab with a positive and friendly relationship between lab members.

Also, I owe the success of my project to my co-advisor Dr. Soo Rin Kim. She helped me develop my basic concept and lab skills in this field, and gave me tremendous help not only in research but also in other areas. As her first student, I received much more opportunities than any normal graduate students to get involved in different research projects and attend science conferences.

Many thanks to the Soo group members, who shared benches and jokes with me. It was their care and help that lit those cold nights when I worked late in the lab. I would like to thank Uros for helping me get familiar with basic lab skills and discussing experiment designs with me. Moreover, I would like to thank Anastashia, Clarissa and Matthew for helping me do cloning and fermentation. It was such a memorable moment when we got together and made handicraft for Soo Rin's leave, that I would never forget it.

Next, I want to thank all the Jin Lab members. Dr. Na Wei introduced me into this lab during my summer visiting and helped me realize the beauty of microbial research. Dr. Zhang provided me the place to stay and drove me to the lab every day when I was waiting for my apartment. He is like a big brother, who not only gave me a lot of suggestions for the experiment and brought me out to try different restaurants. Likewise, two female lab mates, In Iok and Heejin, always answered my questions about both research and courses, and drove me home

during nights. Especially, I want to thank In Iok for her food, which provided me with energy and happiness. Furthermore, I enjoyed and appreciated the discussion and cooperation with Stephan and Suryang. They are both talented and hard-working researchers. Also, I would like to thank Eun-Joong for his kind and patient guidance. He gave me many crucial suggestions on both research and career choice. Additionally, I would like to thank other lab members, including Sonny, Jingjing, Lahiru, Josh, Panchalee, Tim, Seungoh, Pengfei and Hong. I could hardly finish my research without all their help.

The sincere support from my friends in UIUC was another important factor that helped me go through all the hardship during my master's study. No matter how terribly I failed for my experiment, I could easily gain morale after chatting and hanging out with them. Notably, I would like to thank Zhou Zhong. She accompanied me to face all the difficulties and challenges from the time when I began to apply to the master program. It is she who stands by me no matter what happens.

Finally, I want to give my sincere thanks to my parents. It is extremely hard for them to send their only child to study abroad, but they never complain about the lack of my company. Instead, they support me to pursue my dream and always encourages me to face new challenges.

TABLE OF CONTENTS

CHAPTER 1: THESIS OVERVIEW 1
1.1. Study for improving xylose metabolism 1
1.2. Study for the co-fermentation of glucose and xylose 1
CHAPTER 2: PHO13 DELETION-INDUCED TRANSCRIPTIONAL ACTIVATION PREVENTS SEDOHEPTULOSE ACCUMULATION DURING XYLOSE METABOLISM IN ENGINEERED *SACCHAROMYCES CEREVISIAE* 3
2.1. Introduction 4
2.2. Materials and methods 6
2.2.1 Strains and culture conditions 6
2.2.2. Metabolite extraction 6
2.2.3. GC-TOF/MS and statistical analysis 7
2.2.4. NMR analysis 8
2.2.5. Protein expression and purification 9
2.2.6. Phosphatase assay 9
2.2.7. Strain construction using the CRISPR-Cas9 based genome editing system (using *TAL1* promoter substitution as an example) 9
2.2.8. RT-qPCR 11
2.3. Results 11
2.3.1. NMR analysis of the global metabolic response upon *pho13Δ* 11
2.3.2. GC-TOF/MS analysis of the global metabolic response upon *pho13Δ* 12
2.3.3. Manipulation of *TAL1* expression levels using the transcriptome- and Cas9-guided promoter substitution technique 13
2.3.4. Increase in *TAL1* expression leads to lower sedoheptulose accumulation and improved xylose metabolism 14
2.3.5. *GND1* overexpression does not augment xylose metabolism 15
2.3.6. Phosphatase activity of Pho13 on various substrates 16
2.4. Discussion 16
2.5. Tables 20
2.6. Figures 21

2.7. Supplementary materials 28
CHAPTER 3: ENGINEERING *SACCHAROMYCES CEREVISIAE* TO CO-FERMENT GLUCOSE AND XYLOSE BY MUTANT *GAL2* TRANSPORTERS 37
3.1. Introduction 38
3.2. Materials and methods 40
3.2.1. Strains and culture conditions 40
3.2.2. Plasmids and strains construction 41
3.2.3. HPLC analysis 41
3.3. Results 42
3.3.1. Construction and characterization of the sugar-transport-deficient *Saccharomyces cerevisiae* strain 42
3.3.2. Restoration of xylose and glucose fermentation ability by introducing Gal2 transporter 43
3.3.3. Overexpression of Gal2-N376V in SR8D8 and the co-fermentation of glucose and xylose by SR8D8 41K-GAL2-V 44
3.3.4. Overexpression of Gal2-N376F in SR8D8 and the co-fermentation of glucose and xylose by the co-culture system 44
3.3.5. The combination effect of Gal2-N376F and Gal2-N376V in SR8D8 45
3.4. Discussion 46
3.5. Tables 49
3.6. Figures 50
3.7. Supplementary materials 56
CHAPTER 4: CONCLUSIONS AND FUTURE WORK 64
4.1. Conclusions 64
4.1.1 Study for improving xylose metabolism 64
4.1.2. Study for the co-fermentation of glucose and xylose 65
4.2. Future work 66
Chapter 5: BIBLIOGRAPHY 68

CHAPTER 1: THESIS OVERVIEW

1.1. Study for improving xylose metabolism

In this study, we try to understand the mechanism of *pho13Δ* for improving xylose metabolism. Several independent studies reported that *pho13Δ* was beneficial for xylose metabolism (Kim et al., 2013c; Van Vleet et al., 2008). However, Pho13 is a non-specific phosphatase (Kaneko et al., 1989), which shows little connection to xylose metabolism. By using metabolomics approaches, we identified the most prominent metabolic changes caused by *pho13Δ*, which are the significant reduction of sedoheptulose-7-phosphate (S7P), an intermediate of PPP, and its dephosphorylation product, sedoheptulose. Interestingly, sedoheptulose-7-phosphate is a substrate of transaldolase (Tal1), the expression of which increased after *pho13Δ* (Kim et al., 2014). Therefore, we developed the Cas9-guided promoter substitution method to modulate *TAL1* expression level and examined its relation to the reduction of sedoheptulose-7-phosphate and sedoheptulose. Finally, integration of metabolic changes with transcriptional responses revealed that *TAL1* upregulation most significantly contributed to the metabolic and phenotypic changes induced by *pho13Δ*.

1.2. Study for the co-fermentation of glucose and xylose

In the second part of the study, *HXT1-7* and *GAL2* were deleted in an engineered *Saccharomyces cerevisiae* strain with an efficient xylose metabolism pathway, by using the Cas9-guided multiple-gene deletion technique. The resulting strain could not grow on both glucose and xylose while, by complementation with sugar transporters, the strain retained efficient xylose and glucose fermentation ability. This is the first study showing the benefit of the Cas9 technique for rapid construction of the sugar-transport-deficient *Saccharomyces cerevisiae*

strain. Furthermore, by introducing previous reported *GAL2* (Farwick et al., 2014) mutants into our sugar-transport-deficient strain, we examined the characteristics of these two mutant transporters. Specifically, Gal2-N376V was able to support co-fermentation of glucose and xylose solely, while overexpression of Gal2-N376V in our sugar-transport-deficient strain generated a mutant strain with strong selectivity towards xylose, which was applied to build a co-culture system for the co-fermentation of glucose and xylose. Finally, by the combination of these two transporters, we achieved co-fermentation of glucose and xylose with the similar rate as compared to sequential fermentation by the parental strain.

CHAPTER 2: PHO13 DELETION-INDUCED TRANSCRIPTIONAL ACTIVATION PREVENTS SEDOHEPTULOSE ACCUMULATION DURING XYLOSE METABOLISM IN ENGINEERED *SACCHAROMYCES CEREVISIAE*

The content of this chapter is in preparation for submission. I and Sooah Kim were the co-first authors of the paper and Hagit Sorek, Yongsuk Lee, Dukyeol Jeong, Jeong Yun Kim, Eun Joong Oh, Eun Ju Yun, David E. Wemmer, Kyoung Heon Kim, Soo Rin Kim, and Yong-Su Jin, were co-authors. I performed the research with help from the co-authors, and Dr. Yong-Su Jin and Dr. Soo Rin Kim were the directors of the research.

2.1. Introduction

Saccharomyces cerevisiae is one of the most widely used industrial microorganisms because of its excellent fermentation performance under various stress conditions; it can also be easily genetically engineered (Jeffries and Jin, 2004; Olsson and Nielsen, 2000). To facilitate the anticipated transition of current crop-based bioprocesses to sustainable cellulosic processes (Park et al., 2001), metabolic engineering approaches to develop microorganisms capable of fermenting xylose efficiently and rapidly have been undertaken (Kim et al., 2013b). While xylose is one of the two major sugars in most cellulosic biomass hydrolysates, *S. cerevisiae* strains which are currently used for bioethanol production from corn and sugarcane cannot ferment xylose. In order to enable xylose fermentation in *S. cerevisiae*, heterologous xylose-assimilating pathways converting xylose to xylulose-5-phosphate, an intermediate of the native pentose phosphate pathway (PPP), were introduced into *S. cerevisiae* (Billard et al., 1995; Brat et al., 2009; Hahn-Hagerdal et al., 2007; Ho et al., 1998; Jeffries and Jin, 2004; Karhumaa et al., 2007a; Karhumaa et al., 2007b; Kim et al., 2013b; Lee et al., 2014b; Takuma et al., 1991; Tantirungkij et al., 1993).

While initial attempts confirmed the feasibility of fermenting xylose through introducing the heterologous xylose metabolic pathways, yields and productivities of ethanol from xylose were far from commercial use needs. Numerous follow-up studies identified extra genetic perturbations that enhanced xylose fermentation by engineered *S. cerevisiae* (Diao et al., 2013; Hahn-Hagerdal et al., 2007; Hasunuma et al., 2014; Kim et al., 2013b; Kim et al., 2013c; Kuyper et al., 2005a; Lee et al., 2014b; Matsushika et al., 2009; Ni et al., 2007). The step most speculated to be limiting for efficient xylose metabolism was PPP, where xylulose-5-phosphate is metabolized into intermediates of glycolysis, fructose-6-phosphate and glyceraldehyde-3-

phosphate (Diao et al., 2013; Kim et al., 2013b; Matsushika et al., 2009). Indeed, overexpression of genes in the non-oxidative PPP significantly improved the rate of xylose metabolism (Hasunuma et al., 2014; Kuyper et al., 2005a; Latimer et al., 2014; Lu and Jeffries, 2007; Matsushika et al., 2012). Among the PPP genes, *TAL1* is widely accepted to be the most effective target gene for improving xylose metabolism (Kim et al., 2013b; Latimer et al., 2014; Lee et al., 2014b; Ni et al., 2007; Walfridsson et al., 1995).

In addition to the aforementioned rational approach, laboratory evolution and random mutagenesis have been performed to overcome unknown limiting factors of xylose metabolism (Kim et al., 2013c; Kuyper et al., 2005b; Liu and Hu, 2010; Ni et al., 2007; Peng et al., 2012; Sanchez et al., 2010; Sonderegger and Sauer, 2003; Tomitaka et al., 2013; Wisselink et al., 2009). At least two independent studies observed that evolved mutants capable of metabolizing xylose efficiently acquired a mutation in the *PHO13* gene, which encodes an - alkaline phosphatase (Kim et al., 2013c; Van Vleet et al., 2008). Several follow-up studies confirmed that deletion of *PHO13* (*pho13Δ*) significantly improved xylose fermentation without impairing glucose fermentation capability (Fujitomi et al., 2012; Kaneko et al., 1989; Kim et al., 2013c; Kim et al., 2014; Lee et al., 2014b; Li et al., 2014; Ni et al., 2007; Sakihama et al., 2015; Van Vleet et al., 2008).

A very recent study reported that the Pho13 enzyme is involved in transcriptional regulation of the PPP (Kim et al., 2014). Transcriptome analysis revealed that nine genes were significantly upregulated by *pho13Δ* and six of them were directly related to either PPP (*SOL3*, *GND1*, *TAL1*) or NADPH regeneration (*GCY1*, *GOR1*, *YEF1*). Interestingly, the transcription factor *STB5*, activated under oxidative stress, was necessary for the transcriptional changes

induced by *pho13Δ*. However, neither the exact mechanism of transcriptional regulation nor the biological significance of Pho13 has been entirely understood.

Using metabolomics approaches, the present study examined metabolic changes elicited by *pho13Δ* in engineered yeast cells grown on xylose-containing medium. Notably, we detected significantly lowered levels of sedoheptulose-7-phosphate (S7P), an intermediate of PPP, and its dephosphorylation product in the *pho13Δ* mutant as compared to the parental strain. Moreover, integration of metabolic changes with transcriptional responses revealed that *TAL1* upregulation most significantly contributed to the metabolic and phenotypic changes induced by *pho13Δ*.

2.2. Materials and methods

2.2.1 Strains and culture conditions

All strains and plasmids used in this study were listed in Table 2.3. Yeast strains were first grown in 5 mL of YP medium (10 g/L yeast extract, 20 g/L Bacto peptone) containing 20 g/L glucose aerobically at 30°C for 24 hours. Then it was harvested and washed twice with sterile water. For fermentation experiments, the initial cell densities were adjusted to around OD = 1 (optical density at 600 nm), which is about 0.47 g/L dry cell weight. Fermentation experiments were conducted under oxygen-limited condition in 125 mL flasks containing 25 mL medium at 30°C and 100 rpm.

2.2.2. Metabolite extraction

Metabolite extraction was conducted with slight modifications to previously described (Kim et al., 2013a). Briefly, cells were collected by fast vacuum-filtering 1 mL of yeast strains at mid-exponential growth phase (dependent on cell density) through a 30 mm diameter nylon

membrane filter (0.45 μm pore size; Whatman, Piscataway, NJ) and then washed with 5 mL of water. The filter containing the cells were quickly submerged into 10 mL of acetonitrile/water mixture (1:1, v/v) at -20°C and the extraction mixture of cells and solvent was then transferred into liquid nitrogen. The extraction mixture was thawed on ice and vortexed for 3 min. After centrifuging at 16100 g for 5 min at 4°C, the supernatant was collected and concentrated until completely dried in a vacuum concentrator (Labconco; Kansas City, MO).

Prior to GC-TOF/MS analysis, the metabolite samples were derivatized by methoxyamination and trimethylsilylation. For methoxyamination, 5 μL of methoxyamine hydrochloride in pyridine (40 mg/mL; Sigma-Aldrich, St. Louis, MO) was added to the samples and incubated for 90 min at 30°C. For trimethylsilylation, 45 μL of *N*-methyl-*N*-trimethylsilyltrifluoroacetamide (Fluka, Buchs, Switzerland) was added to the samples and incubated for 30 min at 37°C. Finally, fatty acid methyl ester mixture (C08 – C30) was added to the derivatized samples as the internal retention index marker.

2.2.3. GC-TOF/MS and statistical analysis

GC-TOF MS analysis was conducted using an Agilent 7890B GC equipped with a Pegasus HT TOF MS (Leco, St. Joseph, MI). A 1 μL aliquot of derivatized samples was injected into the GC in a splitless mode and separated on an RTX-5Sil MS column (30 m × 0.25 mm, 0.25 μm film thickness; Restek, Bellefonte, PA) with an integrated guard column (10 m × 0.25 mm, 0.25 μm film thickness; Restek, Bellefonte, PA). The initial oven temperature was set at 50°C for 1 min, and then ramped at 20°C/min to a final temperature of 330°C, held for 5 min. The temperatures of ion source and transfer line were set at 250°C and 280°C, respectively. An

electron impact of 70eV was used for ionization. The mass spectra of metabolites were obtained in the mass range of 85 – 500 m/z at an acquisition rate 17 spectra/s.

The preprocessed raw data were obtained using LECO Chroma TOF software (ver. 4.50; St. Joseph, MI) and the further processed data were obtained using BinBase, in-house database (Kim et al., 2013a; Lee do and Fiehn, 2008; Lee et al., 2014a). The statistical analysis of processed data was performed using Statistica (ver. 7.1; StatSoft, Tulsa, OK) and MultiExperiment Viewer (Dana-Farber Cancer Institute, Boston, MA) (Denkert et al., 2008; Saeed et al., 2006)

2.2.4. NMR analysis

Metabolite extract samples were dissolved in 0.5 mL of NMR buffer (0.5 mL D_2O with 100 mM sodium phosphate and 0.02 mM DSS as internal standard). All NMR spectra were recorded at 25°C on a Bruker Avance 600 MHz using a 5 mm TXI Cryoprobe. 1D ^1H NMR spectra were acquired using a standard Bruker noesypr1d pulse sequence. Experiments were acquired with 1024 scans of 64K data points with a spectral width of 8 kHz, an acquisition time of 3.9 s, and a recycle delay of 1 s. Metabolite identification and assignment were performed with the support of 2D NMR experiments: total correlation spectroscopy (TOCSY); heteronuclear single quantum correlation (HSQC); and heteronuclear multiple bond correlation (HMBC). Interpretation was done with the assistance of information from the Biological Magnetic Resonance Bank (BMRB) (Ulrich et al., 2008) and Chenomx NMR software (version 7.6) (Chenomx). Bruker Topspin 3.2 software was used to process and analyze all spectra.

2.2.5. Protein expression and purification

The *PHO13* gene was amplified from *S. cerevisiae* D452-2 genomic DNA and ligated with the pETDuet-1 plasmid using BamHI and SalI restriction enzyme sites, resulting in the pETDuet-1_*ScPHO13* plasmid. *E. coli* BL21 transformant of the plasmid was grown in LB broth with 100 μg/mL ampicillin and the Pho13 recombinant protein with N-terminal His-tag was purified by Ni-NTA affinity column following the manufacturer's instructions (Qiagen 30600, Valencia, CA).

2.2.6. Phosphatase assay

The protein concentration of purified Pho13 solution (1.73 mg/mL) was determined by BCA protein assay kit (Pierce, Rockford, IL). Phosphatase activity was tested in 200 μL of reaction solution containing 1 μg enzyme, 0.1 mM substrate, and 50 mM HEPES-K buffer (pH 7.5). After incubation for 30 min at 25ºC, 80 uL of the reaction solution or diluted one was used to quantify the amount of free phosphates by Malachite green phosphate assay kit as the manufacturer's instructions (BioAssay Systems POMG-25H, Hayward, CA). Reaction solution without a substrate served as a negative control and free phosphate contamination in each substrate solution has been subtracted from the total phosphate concentration. Phosphatase activity was expressed as μmol/min/mg.

2.2.7. Strain construction using the CRISPR-Cas9 based genome editing system (using *TAL1* promoter substitution as an example)

The pRS41N plasmid harboring the Cas9 cassette was constructed by switch the *TRP1* selection marker of p414-TEF1$_P$-Cas9-CYC1$_T$ (Plasmid #43802, Addgene Inc) with *NAT1*.

For construction of guide RNA (gRNA) expressing plasmid, vector pRS42K plasmid was linearized with EcoRV, then treated with rSAP and finally ligated with different singular gRNA expressing cassette. For designing the gRNA, a PAM (NGG) sequence around 57 bp upstream of the starting codon of *TAL1* was chosen and then 20 bp target sequence upstream of the PAM sequence was determined for guide RNA. The 20 bp guide sequences were designed as described in Table 2.4. And the gRNA cassettes were obtained from IDT (Coralville, IA) as gBlocks gene fragments with 5' phosphorylated ends. After guided RNA plasmids were obtained, they were treated with BamHI and SalI to check the presence of insert.

Around 500 to 700 bp promoter regions of four target genes were flanked with homologous sequence of the promoter region of *TAL1* as PCR amplified as donors. When determining the optimal length for the promoter, introducing ORFs from other genes abutting our target promoters were avoided. All the donor DNA was amplified by using primer as shown in Table 2.5. The primers for donor amplification were totally 60 bp long with around 20 bp homologous region of the template target promoter and round 40 bp homologous region from the *TAL1* promoter.

The pRS41N-Cas9 plasmid was introduced into parental strain SR7 and the selected colonies were plated on YPD agar containing 120 µg/mL nourseothricin (clonNAT). Then SR7 pRS41N-Cas9 strain was transformed with both guide RNA plasmid and donor DNA. Next colonies were selected from YPD plate containing both 120 µg/mL nourseothricin and 300 µg/mL geneticin (G418) and confirmed by yeast colony PCR and sequencing with the primers mentioned in Table 2.5, according to the presence of right insertion.

2.2.8. RT-qPCR

RNA was extracted from cells growing in the exponential phase as previously described (Kim et al., 2014). cDNA was generated from 1 µg purified RNA by using iScript cDNA Synthesis Kit (Bio-Rad, Hercules, CA, USA) in a 20 µL reaction. The producing solution was diluted to 100 µL, and 5 µL of diluted solution was used for quantitative PCR by using iQ SYBR Green Supermix (Bio-Rad, Hercules, CA, USA) in a 96-Well plate. All the primers (Table 2.5) for qPCR were designed by using the IDT PrimerQuest program and obtained from IDT. The qPCR was conducted on a LightCycler 480 apparatus (Roche, Basel, Switzerland). The *ACT1* gene was used as a housekeeping gene. The comparative threshold cycle (C_T) method (the $\Delta\Delta C_T$ method) was used to calculate the RT-qPCR results (Kim et al., 2014).

2.3. Results

2.3.1. NMR analysis of the global metabolic response upon *pho13Δ*

An engineered *S. cerevisiae* strain capable of fermenting xylose at a suboptimal level (SR7) and its *PHO13* deletion mutant (SR7 *pho13*Δ) were constructed in our prior study (Kim et al., 2013c). When the two engineered strains were grown on xylose-containing medium as the sole carbon source, the *pho13*Δ mutant grew 5- fold faster than the control strain (Kim et al., 2013c). To investigate the metabolic changes resulting from *pho13Δ*, we performed metabolic profiling of the yeast intracellular metabolites using NMR. The NMR spectra showed that there were substantial differences between the SR7 strain and the *pho13*Δ mutant, as seen in the 1D aliphatic region spectra (Fig. 2.8) and on comparing their 2D HSQC spectra (Fig. 2.1A and 2.1B). Among the signals that contribute to the differences, those at δ_H 4.29 and 4.07 ppm were the most prominent in the metabolites from the SR7 strain (Fig. 2.8A), whereas the 2D HSQC

spectrum showed five dominant peaks at δ_H/δ_C 4.29/78.1, 4.07/78.5, 3.83/75.2, 3.75/83.0, and 3.57/65.3 ppm (Fig. 2.1A). The structure of the compound was resolved by interpreting the two-dimensional HSQC, TOCSY, and HMBC spectra, as well as reviewing the existing literature on NMR chemical shifts (Ceusters et al., 2013). The TOCSY spectrum revealed that the five additional correlations evident in HSQC are within the same spin system, and the HMBC experiment added long-range CH correlations to an anomeric carbon at δ_C 104.8 ppm. Based on these data, the signals were attributable to α-furanose form of sedoheptulose. The spectra show that sedoheptulose level significantly decreases in the *pho13*Δ mutant.

2.3.2. GC-TOF/MS analysis of the global metabolic response upon *pho13Δ*

For capturing the metabolic changes at higher resolution, the intracellular metabolites of the SR7 strain and the *pho13*Δ mutant were analyzed by GC-TOF/MS after derivatization. A total of 134 metabolites were identified and subjected to hierarchical clustering analysis (HCA) and principal component analysis (PCA). Six replicates of the control strain and the *pho13*Δ mutant were clearly discriminated as clustered in the heat map (Fig. 2.9), and as shown in the score plot (Fig. 2.1C). Based on principal component (PC) 1, the levels of 70 metabolites including sedoheptulose and sedoheptulose-7-phosphate (S7P) were low in the *pho13*Δ mutant, whereas the levels of 64 other metabolites detected were higher compared to the corresponding metabolite levels in the control strain (SR7). The top 30 metabolites contributing toPC1 and PC2 were listed in Table 2.2. A 98% reduction in sedoheptulose was the most prominent change induced by *pho13Δ* (Fig. 2.1D), corroborating the results from the NMR analysis.

2.3.3. Manipulation of *TAL1* expression levels using the transcriptome- and Cas9-guided promoter substitution technique

Significant reduction of sedoheptulose (98%) and S7P (83%) suggested that related metabolic pathways are affected by *pho13Δ*. Since S7P is a substrate of transaldolase (*TAL1*) in PPP, we reasoned that transaldolase activity might be limiting in the control strain (SR7) when metabolizing xylose as compared to the *pho13*Δ mutant. Indeed, *TAL1* is one of the genes that are up-regulated by *pho13Δ*, as reported in our previous study (Kim et al., 2014).

To test the hypothesis, various xylose-fermenting strains with different *TAL1* expression levels were constructed by replacing the original promoter of *TAL1* with promoters exhibiting discrete levels of transcriptional activity. In order to select the promoters which will be used to replace the original promoter of *TAL1*, we analyzed RNA-seq data published previously (Kim et al., 2014), and identified genes that were constitutively expressed under both glucose and xylose conditions. Based on the abundances of their transcripts, we selected four genes showing approximately 2-fold (*RPS13*), 3-fold (*HFF1*), 8-fold (*TEF2*), and 17-fold (*CCW12*) higher expression levels as compared to the native *TAL1* (Table 2.1). Promoter regions of the selected set of genes were PCR-amplified as donor DNA to repair a double strand break upstream of *TAL1* created by an RNA-guided DNA endonuclease (Cas9) (see Materials and Methods; Fig. 2.2A). Four resulting strains with the replaced promoters of *TAL1* have genetic backgrounds identical to the original SR7 strain because Cas9-based genome editing is highly-specific to a designed target. To confirm differential expression of *TAL1* via the Cas9-guided promoter substitution strategy, *TAL1* expression levels in the four promoter-replaced mutants and the original SR7 strain were measured by RT-qPCR. As shown in Table 2.1 and Figure 2.2B, the four mutants had elevated expression levels of *TAL1* with marginal differences compared with

the expected values: 4-fold (*RPS13$_P$-TAL1*), 3-fold (*HFF1$_P$-TAL1*), 9-fold (*TEF2$_P$-TAL1*), and 20-fold (*CCW12$_P$-TAL1*). Moreover, theoretical promoter strength (relative to transcript abundance of the corresponding gene) and the empirical values (transcript abundance of the engineered *TAL1* gene) were well correlated (Fig. 2.10).

2.3.4. Increase in *TAL1* expression leads to lower sedoheptulose accumulation and improved xylose metabolism

To investigate phenotypic and metabolic changes in response to the elevated expression levels of *TAL1*, xylose fermentation profiles by the four mutants and the parental strain (SR7) were examined. Cell growth, xylose consumption as well as ethanol production improved as the expression levels of *TAL1* increased (Fig. 2.3). Moreover, intracellular concentrations of sedoheptulose and S7P were negatively correlated with *TAL1* expression levels (Fig. 2.4A and Fig. 2.4B). This result suggests that overexpression of *TAL1* might lead to decrease in sedoheptulose accumulation and increase in xylose fermentation of engineered *S. cerevisiae*. Taken together with previous reports, we concluded that transaldolase (encoded by *TAL1*) was indeed the primary rate-limiting step of xylose metabolism in engineered *S. cerevisiae,* and the limitation could be overcome by *pho13Δ* via transcriptional activation of *TAL1*.

However, the extent of the metabolic changes induced by *pho13Δ* could not be attributed to the same level of *TAL1* upregulation alone. Specifically, the *pho13*Δ mutant showed only 3-fold upregulation of *TAL1* but it exhibited significantly higher xylose consumption rates and lower intracellular sedoheptulose concentrations than the mutant strain with 4-fold *TAL1* overexpression (SR7 *RPS13$_P$-TAL1*), which was created by the promoter replacement strategy

(Table 2.1). Excessive levels of *TAL1* overexpression (9-fold and 20-fold) were necessary to achieve the xylose consumption rates as high as the *pho13Δ* strain (Fig. 2.4B).

2.3.5. *GND1* overexpression does not augment xylose metabolism

As the equivalent overexpression of *TAL1* by promoter replacement did not lead to similar performance of xylose fermentation by the *pho13*Δ mutant, we hypothesized that other PPP genes upregulated by *pho13Δ* might be responsible for *pho13Δ*-induced metabolic and phenotypic changes: i.e. reduced sedoheptulose accumulation and improved xylose metabolism. Thus, we investigated the overexpression effect of *GND1*, which showed the highest upregulation (15-fold) in response to *pho13Δ* among all PPP genes (Kim et al., 2014). A strain overexpressing *GND1* was constructed by changing its promoter to $TPI1_P$ (see Materials and Methods), and the resulting strain (SR7 $TPI1_P$ -*GND1*) exhibited a 6-fold increase in *GND1* expression compared with the control (Fig. 2.5A). However, no positive phenotypic changes were observed in the *GND1*-overexpressing mutant during growth on xylose-containing medium (Fig. 2.5B and C). This result suggests that *GND1* upregulation alone does not yield the metabolic changes that are observed in the *pho13Δ* strain.

Interestingly, when we measured the PP pathway genes expression levels after *TAL1* overexpression, we found that *ZWF1*, *SOL3* and *TKL1* had the similar expression levels in *TAL1* overexpression strain (SR7 *CCW12p-TAL1*) and parental strain, in both glucose and xylose condition. However, *GND1* expression level was induced in xylose condition but not glucose condition (Fig. 2.11).

2.3.6. Phosphatase activity of Pho13 on various substrates

As the upregulation of PPP genes did not sufficiently explain the enhanced xylose fermentation upon *pho13Δ*, we hypothesized that the catalytic activity of Pho13 might be detrimental to xylose metabolism in engineered *S. cerevisiae*. Because Pho13 is known as alkaline phosphatase, we examined its phosphatase activity on various intermediates of xylose-metabolic pathway (Fig. 2.6). Interestingly, Pho13 exhibited non-specific phosphatase activity on all intermediates of PPP including S7P, while its phosphatase activity on glycolytic intermediates (glucose-6-phosphate and fructose-6-phosphate) was negligible. This result suggests that Pho13 might be responsible for the accumulation of sedoheptulose by dephosphorylating S7P during the xylose fermentation by the SR7 strain. Owing to low substrate specificity, it was speculated that Pho13 phosphatase activity on S7P might be significant only when S7P levels are extremely high during xylose metabolism in a strain with limited transaldolase activity.

2.4. Discussion

Application of omic approaches has become immensely popular in the area of metabolic engineering (Dromms and Styczynski, 2012; Han et al., 2011; Park et al., 2005; Vemuri and Aristidou, 2005). The present study is another example of using metabolomics for strain development, especially for engineering xylose-fermenting *S. cerevisiae*. In previous studies, glucose- and xylose-metabolizing engineered yeast strains were compared using metabolomics (Matsushika et al., 2013; Senac and Hahn-Hagerdal, 1990). Numerous differences in catalytic and signaling pathways were identified between glucose and xylose conditions. In this study, we captured metabolic differences between an efficient xylose-fermenting strain (SR7 *pho13Δ*) and a poor xylose-fermenting strain (SR7) under the same conditions. Both analytical methods—

NMR or GC-TOF/MS—used identified sedoheptulose as the most significantly variable metabolite between the two differently performing strains. The results suggested that the most limiting step of xylose metabolism might be transaldolase (encoded by *TAL1*). Indeed, overexpression of *TAL1* in the low-efficiency strain resulted in dramatic improvement of xylose fermentation capability, comparable to that of the high-efficiency strain. Although the *TAL1* is already known to be an important overexpression target for improving xylose metabolism, our study revealed three novel findings relevant to this field of study.

First, the present study was a follow up to our previous evolutionary engineering work (Kim et al., 2013c), and we successfully undertook systems biology approaches to identify molecular mechanisms responsible for the evolved phenotypes. Evolutionary engineering is one of the most effective metabolic engineering strategies as demonstrated in many studies (Farwick et al., 2014; Kim et al., 2013c; Kuyper et al., 2005b; Lee et al., 2014b; Liu and Hu, 2010; Peng et al., 2015; Peng et al., 2012; Sanchez et al., 2010; Sonderegger and Sauer, 2003; Wisselink et al., 2009). Hence, the best xylose-fermenting strains developed thus far have been isolated after long-term exposure to xylose in either a chemostat or consecutive batch cultures (Kim et al., 2013c; Kuyper et al., 2005b; Lee et al., 2014b; Liu and Hu, 2010; Runquist et al., 2010; Sanchez et al., 2010; Zhou et al., 2012). However, not many studies have attempted to elucidate a detailed mechanism for improved phenotypes of their evolved mutants. The functions of the gene target (*PHO13*) that was identified by genome sequencing of our evolved mutant (Kim et al., 2013c) were investigated using transcriptomics (Kim et al., 2014) and metabolomics, which revealed its novel transcriptional and metabolic activities. We concluded that Pho13 functions as an inhibitory factor in the xylose metabolic pathway as illustrated in Figure 2.7.

Second, the novel biological functions of Pho13 was discovered in our work because the transcriptional and metabolic activities were significant enough to be observed when cells were poorly metabolizing xylose. We think that poor xylose metabolism might mimic certain environmental stresses such as NADPH limitation or sugar phosphate accumulation; thus, understanding these may elucidate the biological significance of Pho13.

Third, we developed transcriptome- and Cas9-guided promoter substitution technology to study the metabolic impact of transcriptional regulation of a target gene (*TAL1*) at high resolution. Previously, manipulating gene expression was limited to the use of single or multi copy plasmids with only a few constitutive promoters. However, episomal overexpression often results in pleiotropic phenotypes owing to selection pressure and/or metabolic burden. In contrast, our promoter substitution approach uses marker-free genome editing technology mediated by Cas9 (DiCarlo et al., 2013; Jakociunas et al., 2015; Mans et al., 2015; Ryan and Cate, 2014; Zhang et al., 2014). Because selection pressures are only required during a genome editing process, once the genome has been mutated, mutants can be tested under the same conditions as their corresponding wild types. Moreover, using the transcriptomic data representative of the strength of each promoter, it was possible to select a wide range of promoters to accurately manipulate expression levels of the target gene, as proven in *TAL1*'s case (Table 2.1). The expression levels of *TAL1* increased by 2–20 folds compared to the wild type strain, and the approach helped us to demonstrate a linear correlation between *TAL1* expression levels and xylose fermentation capability.

Our study investigated metabolic responses to *pho13Δ* in *S. cerevisiae*. Based on the transcriptional changes induced by *pho13Δ*, we concluded that *TAL1* upregulation is primarily initiates the metabolic changes observed in the *pho13Δ* mutant. These changes ultimately result

in significantly improved xylose metabolism in strains expressing a heterologous xylose pathway.

2.5. Tables

Table 2.1. Comparison of *TAL1*-overexpressing mutants with the *pho13*Δ mutant

Gene expression levels measured by RNA-seq				Expression levels of engineered *TAL1* and its impact on xylose metabolism				
Gene	Glucose (RPKM)	Xylose (RPKM)	Relative promoter strength (xylose)	Strains	Relative expression levels of *TAL1*[#]	Relative concentration of S7P*	Relative concentration of sedoheptulose	Specific xylose consumption rate (h^{-1})
TAL1	844	906	1	Control	1	1.000±0.850	1.000±0.261	0.129±0.003
HFF1	2773	3031	3.35	*HFF1p-TAL1*	3.47 ± 0.20	-	-	0.257±0.028
RPS13	3303	2343	2.59	*RPS13p-TAL1*	3.97 ± 0.09	0.910±0.694	0.182±0.098	0.329±0.028
TEF2	6693	7059	7.79	*TEF2p-TAL1*	8.65 ± 1.45	0.169±0.134	0.005±0.002	0.405±0.003
CCW12	14449	15729	17.36	*CCW12p-TAL1*	20.07 ± 1.23	0.121±0.088	0.004±0.001	0.434±0.001
				*pho13*Δ	2.99±0.07	0.172±0.117	0.019±0.006	0.442±0.013

[#]Measured by RT-qPCR using cells grown on xylose-containing medium

*Sedoheptulose-7-phosphate

2.6. Figures

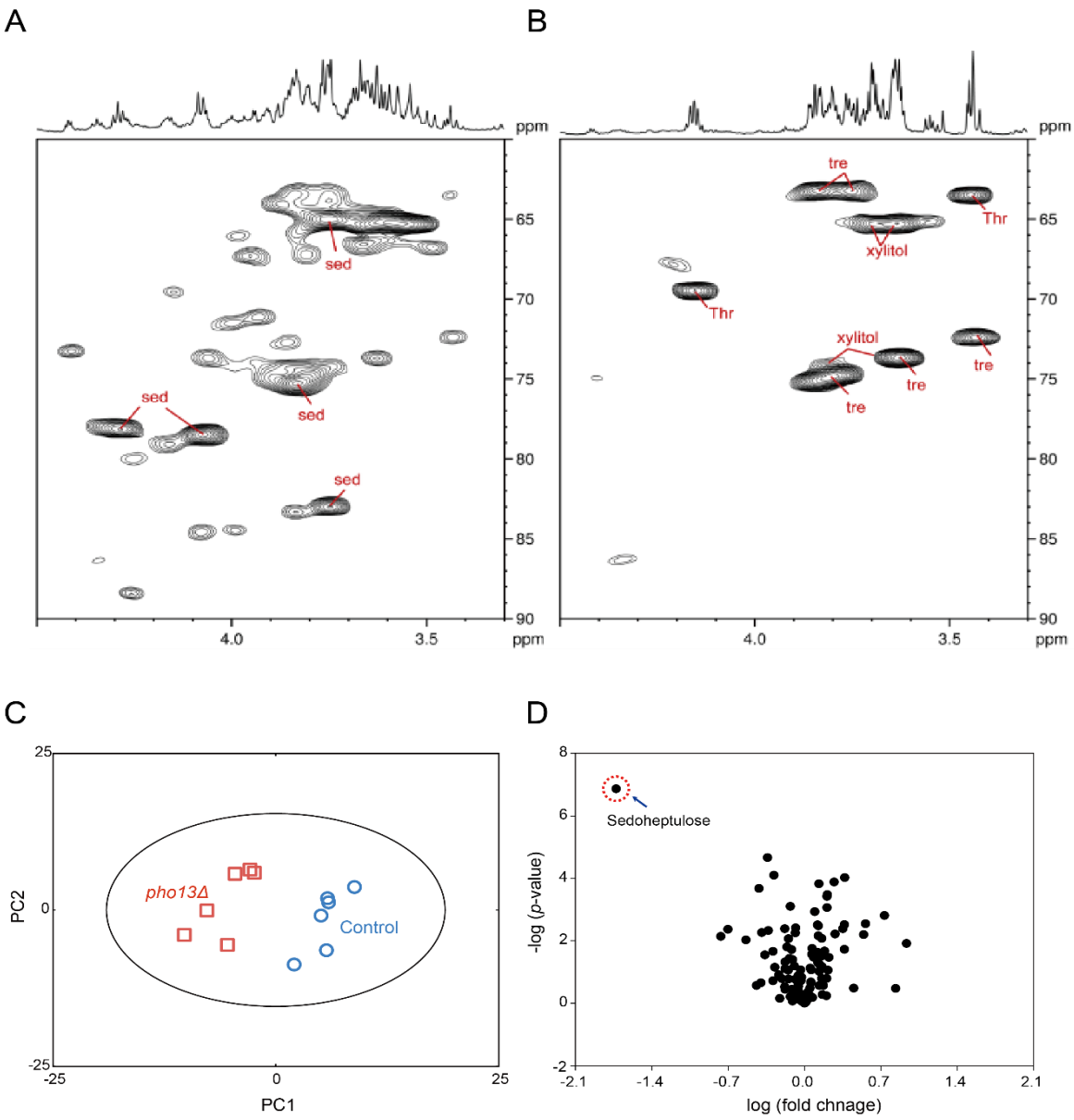

Figure 2.1. Metabolic changes induced by *pho13Δ*. Partial HSQC spectra of the (A) control strain and the (B) *pho13Δ* mutant obtained from NMR analysis shows significant reduction of sedoheptulose by *pho13Δ*. (C) Principle component (PC) analysis of metabolite profiles measured by GC-TOF/MS also shows clear differences between the two strains (score plot), and (D) sedoheptulose was significantly low in the *pho13Δ* mutant. sed, sedoheptulose; tre, trehalose; Thr, threonine.

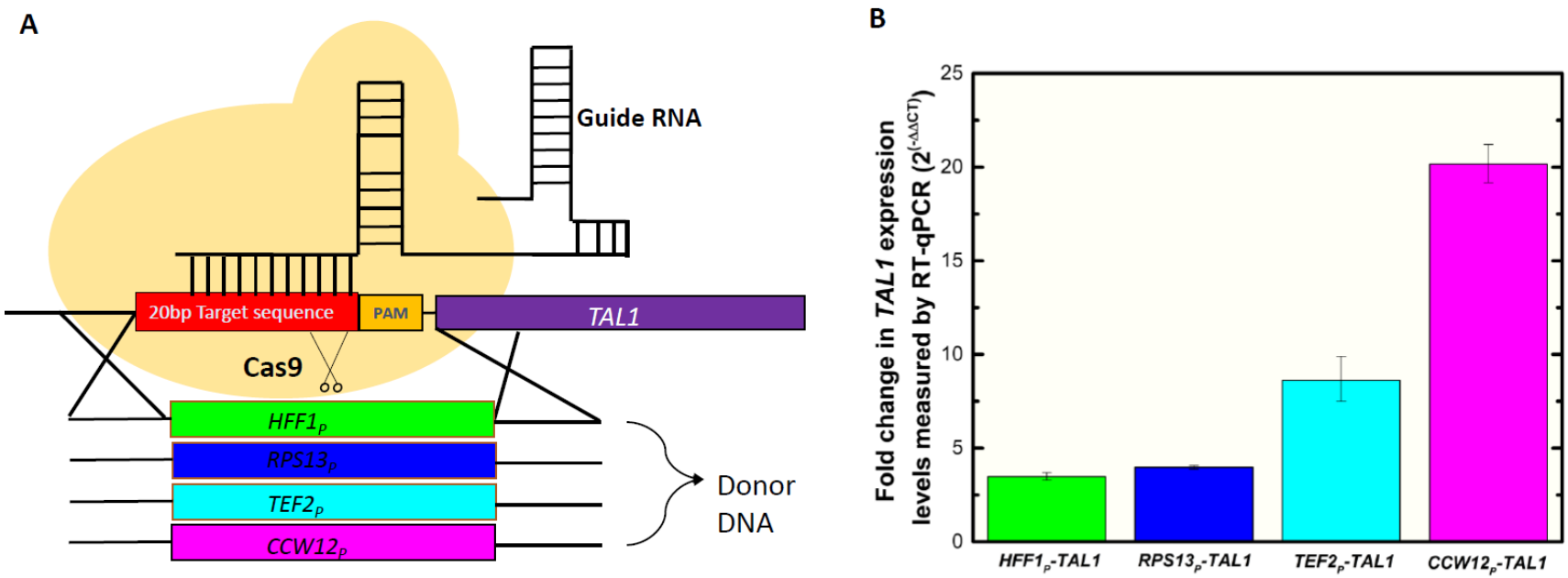

Figure 2.2. Increased *TAL1* expression levels in the mutants constructed using the transcriptome- and Cas9-guided promoter substitution method. (A) An illustration of our promoter substitution strategy; four promoters with different strengths were selected based on transcriptome data, and the selected promoters were inserted upstream of the *TAL1* gene using the Cas9 genome editing technique. (B) Changes in *TAL1* expression levels induced by promoter substitution; cells were grown on xylose-containing medium, and *TAL1* expression levels of the mutants and the control strain were measured by RT-qPCR. Error bars indicate standard deviations of three biological replicates.

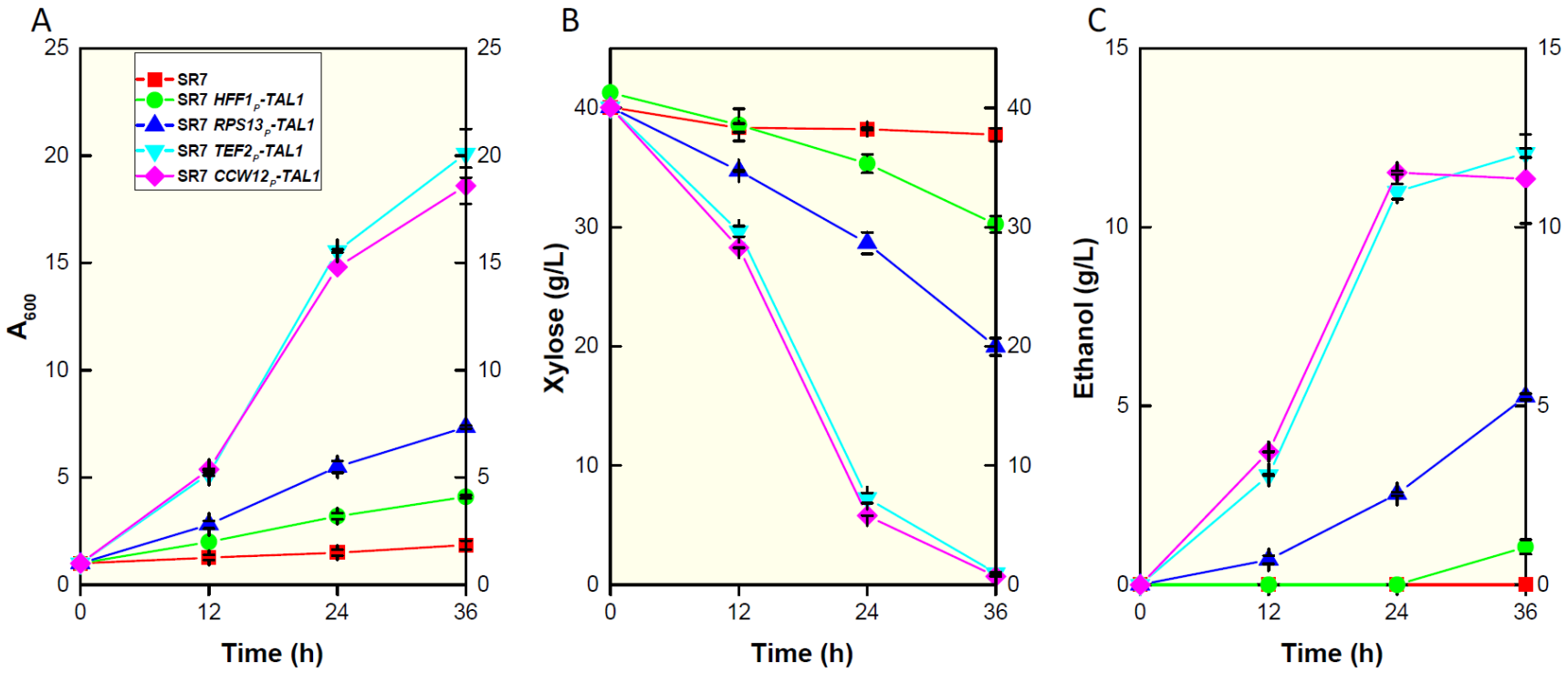

Figure 2.3. Increased rate of xylose metabolism in *TAL1*-overexpressing mutants compared with the control strain (SR7). (A) Cell growth, (B) xylose consumption, and (C) ethanol production were compared. Error bars indicate standard deviations of three biological replicates.

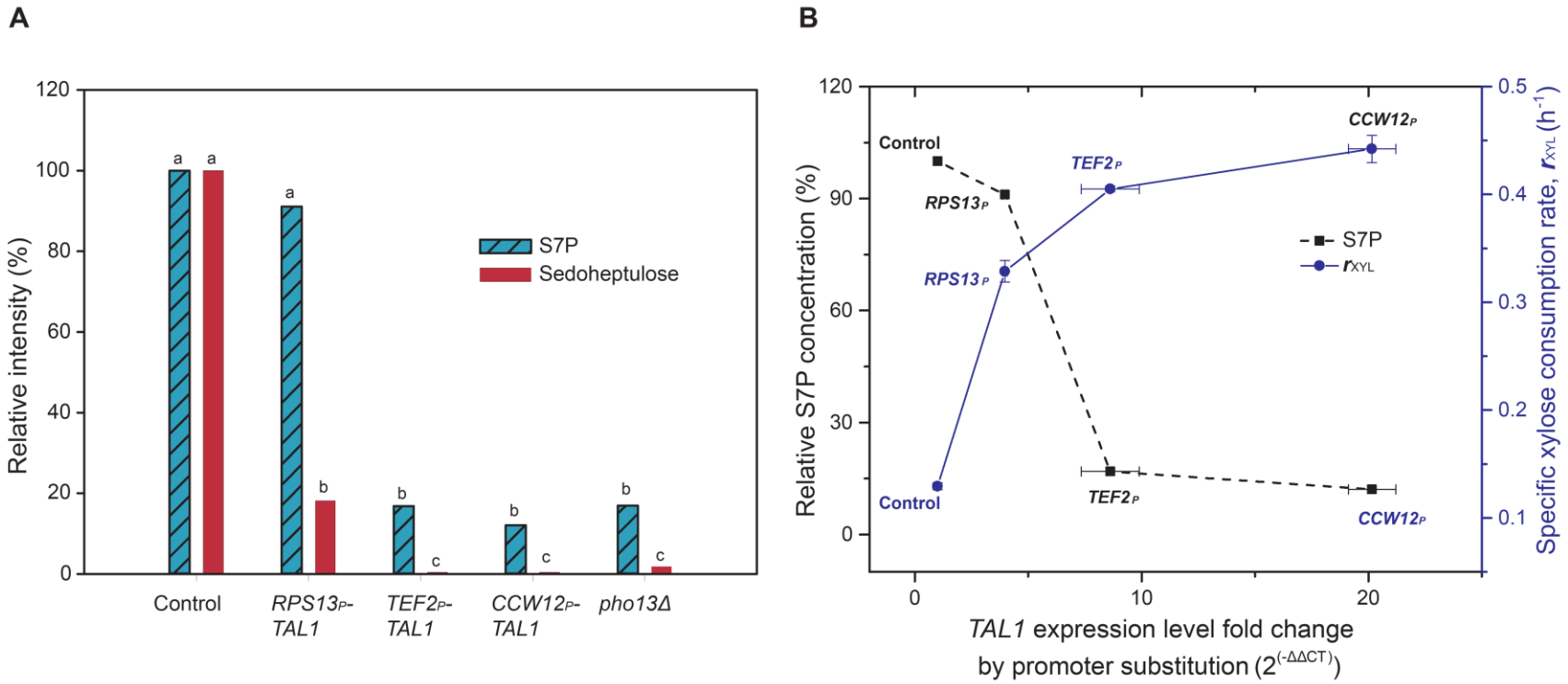

Figure 2.4. Metabolic and phenotypic changes due to *TAL1* overexpression. (A) Reduction in intracellular accumulation of sedoheptulose-7-phosphate (S7P) and sedoheptulose in *TAL1*-overexpressing mutants. The mean of 6 biological replicates represents the metabolite intensity of the mutants relative to that of the control strain (100%). (B) Effect of *TAL1* expression levels on S7P accumulation and xylose consumption rate. *TAL1* expression level negatively correlates with S7P accumulation (black dotted line) but positively correlates with the xylose consumption rate (blue solid line).

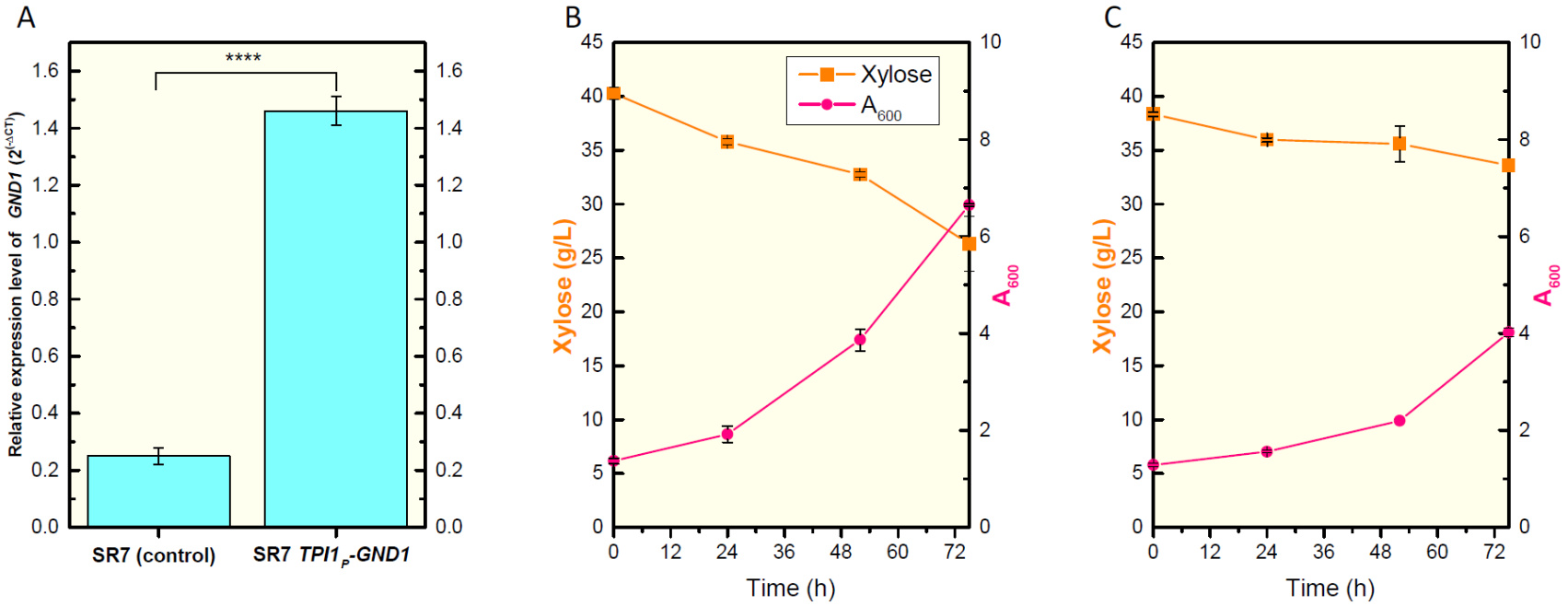

Figure 2.5. Phenotypes of the mutant overexpressing *GND1*. (A) Increased expression level of the *GND1* gene in the *GND1*-overexpressing mutant was confirmed by RT-qPCR. The mutant was constructed by the transcriptome- and Cas9-guided promoter substitution strategy. Growth and xylose consumption of the (B) control strain and the (C) *GND1*-overexpressing mutant were compared.

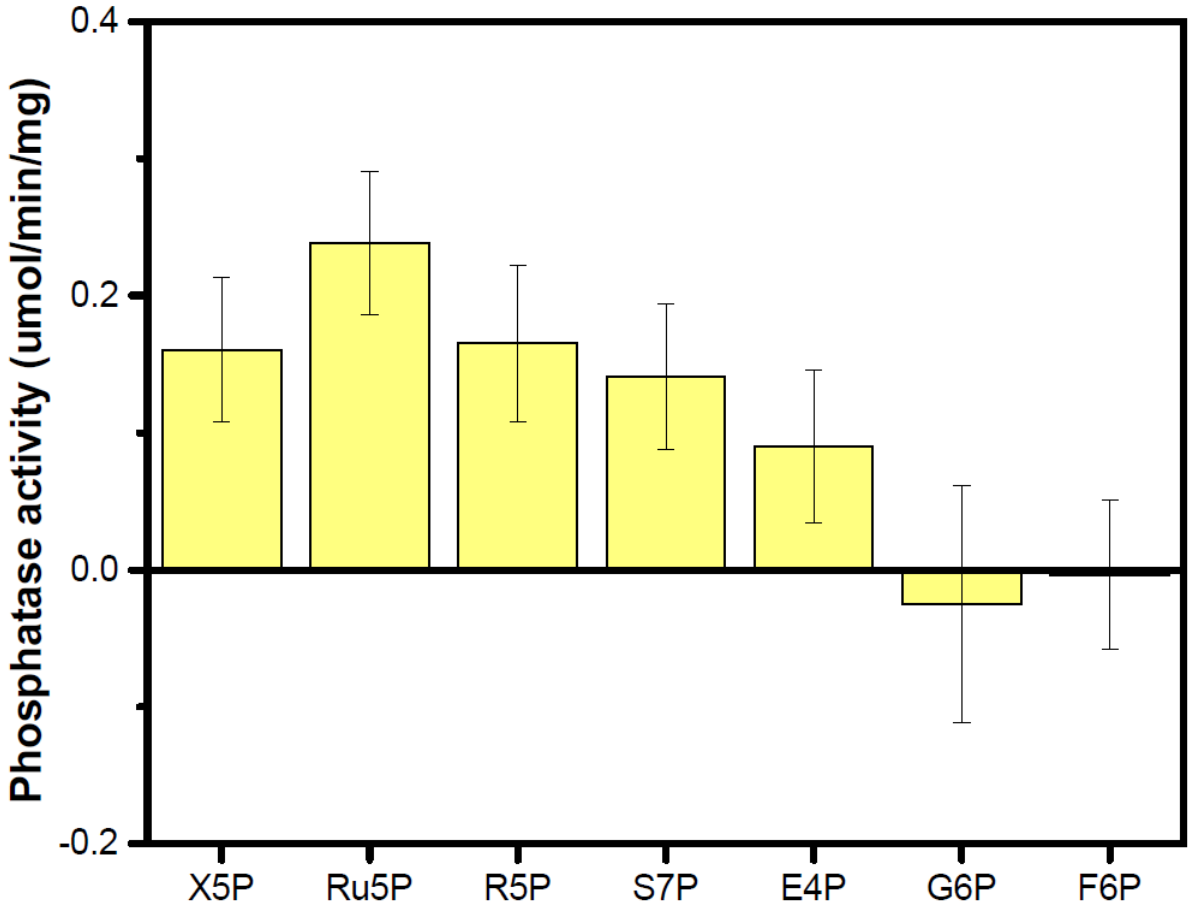

Figure 2.6. *In vitro* phosphatase activity of Pho13 on various sugar phosphates. X5P, xylulose-5-phosphate; Ru5P, ribulose-5-phosphate; R5P, ribose-5-phosphate; S7P, sedeheptulose-7-phosphate; E4P, erythrose-4-phosphate; G6P, glucose-6-phosphate; F6P, fructose-6-phosphate.

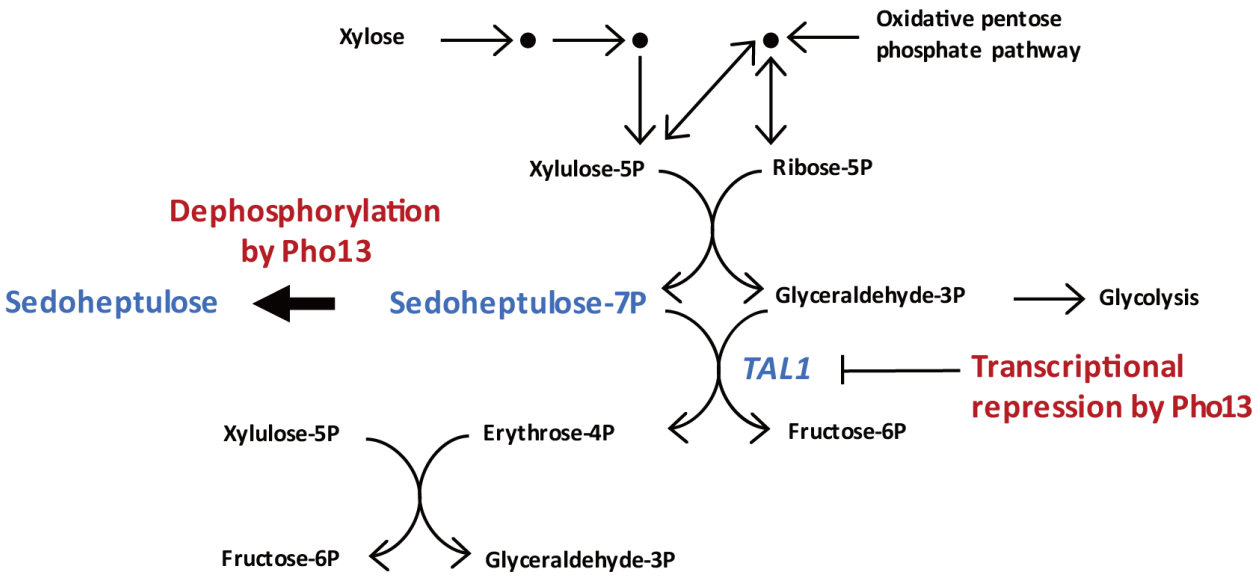

Figure 2.7. Schematic of a putative mechanism for sedoheptulose accumulation during xylose metabolism in engineered *S. cerevisiae*.

2.7. Supplementary materials

Table 2.2. List of major metabolites identified by principle component (PC) analysis

PC1			PC2		
Metabolite	Loading	Fold change*	Metabolite	Loading	Fold change
2-Ketoadipate	0.959	2.187	Carnitine	−0.596	1.009
Sedoheptulose	0.915	−53.324	Palmitic acid	0.822	1.041
Erythrose 4-phosphate	0.906	2.625	Pelargonic acid	0.817	1.013
Benzoate	0.867	1.453	5-Aminovalerate	0.805	1.140
Urea	0.866	2.467	Trehalose 6-phosphate	0.803	1.488
Inosine	0.780	1.915	Octadecanol	0.803	1.026
Cytindine 5-monophosphate	0.761	−4.634	Myristic acid	0.770	1.039
Cholic acid	0.755	2.315	Xylitol	0.765	−1.446
Adipate	0.725	1.411	Threose	0.758	−1.044
Citrate	0.711	3.453	Stearic acid	0.753	1.073
Threitol	0.708	1.408	Melibiose	0.725	1.071
Pyruvate	0.670	1.520	Terephtalate	0.703	−1.021
Sedoheptulose 7-phosphate	0.683	−5.873	Lignoceric acid	0.694	1.025
Methionine	0.688	1.352	Malonate	0.693	1.045
Adenosine	−0.944	1.616	Xylose	0.681	1.104
Ribulose 5-phosphate	−0.925	2.329	Linolenic acid	0.613	1.158
Mannose 6-phosphate	−0.915	5.408	Methylthioadenosine	0.610	1.151
Cellobiose	−0.900	1.357	Trehalose	0.596	1.339
Glutamine	−0.889	1.603	1-Monopalmitin	0.593	1.148
Uridine	−0.879	−1.904	Cysteine	−0.832	1.001
Galactonate	−0.873	1.865	Mannose	−0.717	1.111
Malate	−0.866	1.337	Isoleucine	−0.683	1.064
Xylulose	−0.852	1.315	Glycine	−0.665	1.068
Xanthine	−0.837	−1.144	Tyrosine	−0.651	1.082
Myo-inositol	−0.835	−1.286	3-Phenyllactate	−0.643	1.287
Lactose	−0.806	1.438	Putrescine	−0.641	1.682
Glucose 6-phosphate	−0.785	2.321	Glycerol	−0.635	−1.160
Lactulose	−0.784	8.563	Dihydroxyacetone	−0.633	1.946
Fumarate	−0.773	1.367	Asparagine dehydrated	−0.605	1.031
Uracil	−0.760	−1.238	Threonine	−0.604	1.209

* Fold change was calculated based on the ratio of metabolite intensity of the mutant and the

metabolite intensity of the wild type. If the ratio was less than 1, its negative reciprocal was used.

Table 2.3. List of plasmids and strains used in the study

Plasmid or Strain	Description	Reference
Plasmids		
pETDuet-1_*ScPHO13*	A bacterial plasmid for the expression of *S. cerevisiae PHO13* with a N-terminal His-tag	This study
p41N-Cas9	A single-copy plasmid containing Cas9 and a natMX marker	This study
p42K-gRNA-*TAL1*	A multi-copy plasmid containing a guide RNA and a Geneticin marker	This study
p42H-gRNA-*GND1*	A multi-copy plasmid containing a guide RNA and a Hygromycin B marker	This study
Strains		
E. coli ScPHO13	*E. coli* BL21 pETDuet-1_*ScPHO13*	This study
SR7	*S. cerevisiae* D452-2 with a xylose pathway (*S. stipitis XYL1*, *XYL2*, and *XYL3*)	(Kim et al., 2013c)
SR7 *pho13*Δ	SR7 *pho13*::kanMX	(Kim et al., 2013c)
SR7 p41N-Cas9	SR7 with Cas9 protein expressing plasmid	This study
SR7 *HFF1*$_P$-*TAL1*	SR7 with insertion of a *HHF1* promoter insertion in front of *TAL1* gene	This study
SR7 *RPS13*$_P$-*TAL1*	SR7 with insertion of a *RPS13* promoter insertion in front of *TAL1* gene	This study
SR7 *TEF2*$_P$-*TAL1*	SR7 with insertion of a *TEF2* promoter insertion in front of *TAL1* gene	This study
SR7 *CCW12*$_P$-*TAL1*	SR7 with insertion of a *CCW12* promoter insertion in front of *TAL1* gene	This study
SR7 *TPI1*$_P$-*GND1*	SR7 with insertion of a *TPI1* promoter insertion in front of *GND1* gene	This study

Table 2.4. Guide RNA sequence synthesized as gBlocks (388 bp)

Parts	Sequence	Length (bp)
TAL1 guide RNA		
SNR52 promoter	TCTTTGAAAAGATAATGTATGATTATGCTTTCACTCATATTTATACAGAAACTTGATGTTTTCTTTCGA GTATATACAAGGTGATTACATGTACGTTTGAAGTACAACTCTAGATTTTGTAGTGCCCTCTTGGGCTA GCGGTAAAGGTGCGCATTTTTTCACACCCTACAATGTTCTGTTCAAAAGATTTTGGTCAAACGCTGTA GAAGTGAAAGTTGGTGCGCATGTTTCGGCGTTCGAAACTTCTCCGCAGTGAAAGATAAATGATC	269
TAL1 upstream target	TCTCGAGTATATAATTTTTC	20
Structural crRNA	GTTTTAGAGCTAGAAATAGCAAGTTAAAATAAGGCTAGTCCGTTATCAACTTGAAAAAGTGGCACCG AGTCGGTGGTGC	79
SUP4 terminator	TTTTTTTGTTTTTTATGTCT	20
GND1 guide RNA		
SNR52 promoter	TCTTTGAAAAGATAATGTATGATTATGCTTTCACTCATATTTATACAGAAACTTGATGTTTTCTTTCGA GTATATACAAGGTGATTACATGTACGTTTGAAGTACAACTCTAGATTTTGTAGTGCCCTCTTGGGCTA GCGGTAAAGGTGCGCATTTTTTCACACCCTACAATGTTCTGTTCAAAAGATTTTGGTCAAACGCTGTA GAAGTGAAAGTTGGTGCGCATGTTTCGGCGTTCGAAACTTCTCCGCAGTGAAAGATAAATGATC	269
GND1 upstream target	TGTAGTTTTTGTATAGAAAG	20
Structural crRNA	GTTTTAGAGCTAGAAATAGCAAGTTAAAATAAGGCTAGTCCGTTATCAACTTGAAAAAGTGGCACCG AGTCGGTGGTGC	79
SUP4 terminator	TTTTTTTGTTTTTTATGTCT	20

Table 2.5. List of primers used in the study

Name	Sequence	Description
SOO209	5′-GCC GGATCC AAAAATGACTGCTCAACAAGGT-3′	PHO13_F (BamHI)
SOO210	5′-GCC GTCGAC CTATAACTCATTATTGGTTAAGGT-3′	PHO13_R (SalI)
SOO624	5′-ACTCGCGGGTTTTTCTTTTTTCTCAATTCTTGGCTTCCTCTTCACGCAAAAGAAAACCTT-3′	Donor_*TAL1_CCW12*-F
SOO625	5′-AGCAACCTTTTGTTTCTTTTGAGCTGGTTCAGACATTATTGATATAGTGTTTAAGCGAAT-3′	Donor_*TAL1_CCW12*-R
SOO672	5′-CGGGTTTTTCTTTTTTCTCAATTCTTGGCTTCCTCTTGCTACCTATATTCCACCATAACA-3′	Donor_*TAL1_TEF2*-F
SOO673	5′-CAACCTTTTGTTTCTTTTGAGCTGGTTCAGACATGTTTAGTTAATTATAGTTCGTTGACC-3′	Donor_*TAL1_TEF2*-R
SOO674	5′-ACTCGCGGGTTTTTCTTTTTTCTCAATTCTTGGCTTCCTCTTAATGACGGTCGTTTCACA-3′	Donor_*TAL1_RPS13*-F
SOO675	5′-TGTTAGCAACCTTTTGTTTCTTTTGAGCTGGTTCAGACATTTTGACTGATTGTTGTTGAT-3′	Donor_*TAL1_RPS13*-R
SOO701	5′-ACTCGCGGGTTTTTCTTTTTTCTCAATTCTTGGCTTCCTCTTCTGTTTGCTTTGTTCTGG-3′	Donor_*TAL1_HFF1*-F
SOO702	5′-AGCAACCTTTTGTTTCTTTTGAGCTGGTTCAGACATACTATATTATATTTGTTGCTTGTT-3′	Donor_*TAL1_HFF1*-R
SOO609	5′-CTGATACATATAAACCTGTATTGTTGCCATTACAGAAAAAAGAATGCCCTTCATGCCTCC-3′	Donor_*GND1_ TPI1*-F
SOO610	5′-ACGGCCAAACCAATCAAACCGAAATCAGCAGACATTTTGAATATGTATTACTTGGTTATG-3′	Donor_*GND1_ TPI1*-R
SOO599	5′-GCTATGTCACTAATGATCTCG-3′	*GND1*_confirmation-F (−1000 bp)
SOO618	5′-TGATGGCAGTCCACTTAC-3′	*GND1*_confirmation-R (+802 bp)
SOO626	5′-TTTCTCAATTCTTGGCTTCCTC-3′	*TAL1*_confirmation-F (−104 bp)
SOO676	5′-AGACAATCTAGCATCAACTTCG-3′	*TAL1*_confirmation-R (+342 bp)
SOO613	5′-GCCTTCTACGTTTCCATCCA-3′	RT-qPCR_*ACT1*-F
SOO614	5′-GGCCAAATCGATTCTCAAAA-3′	RT-qPCR_*ACT1*-R
SOO417	5′-CTGCTACTTATGGCTGGAAACT-3′	RT-qPCR_*GND1*-F
SOO418	5′-GGTTCTTCTCTGTAGGCCTTTG-3′	RT-qPCR_*GND1*-R
SOO365	5′-CCTCAAGACTCCACAACTAACC-3′	RT-qPCR_*TAL1*-F
SOO366	5′-ACCATGCTTCTTACCGTATTCC-3′	RT-qPCR_*TAL1*-R

Restriction enzyme sequences are underlined.

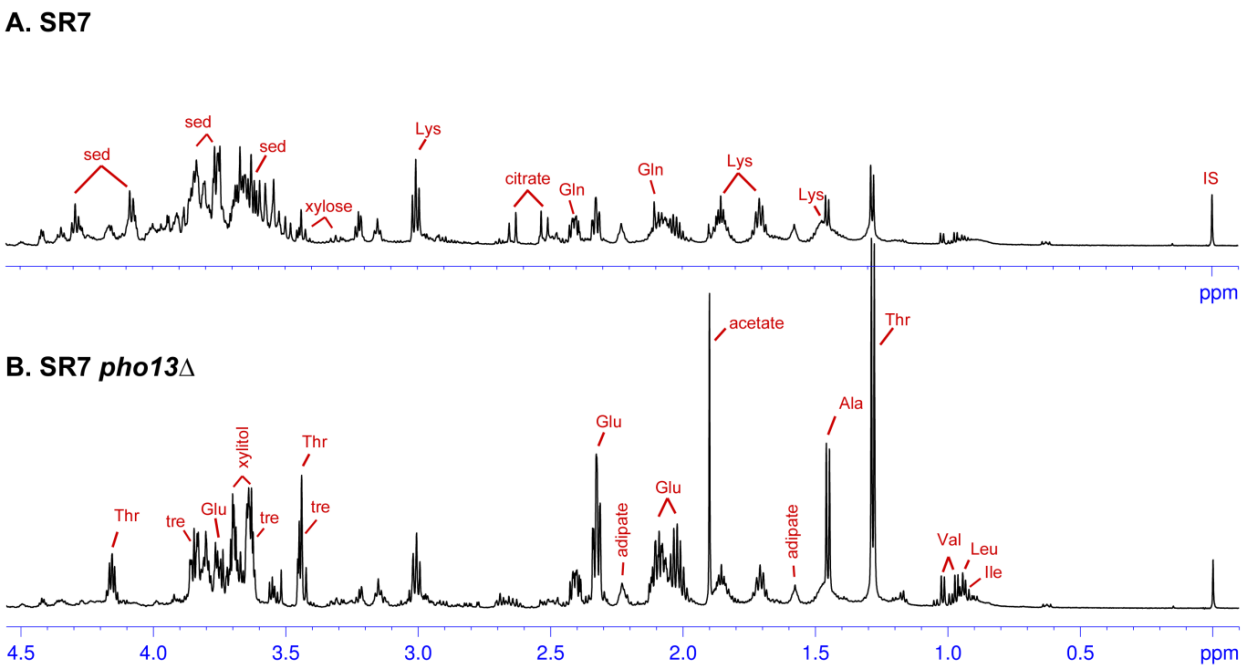

Figure 2.8. Aliphatic regions of the ^{1}H spectra. (A) SR7 and (B) SR7 *pho13Δ*. sed, sedoheptulose; Thr, threonine; tre, trehalose; Lys, lysine; Glu, glutamic acid; Ala, alanine; Val, valine; Leu, leucine; Iie, isoleucine.

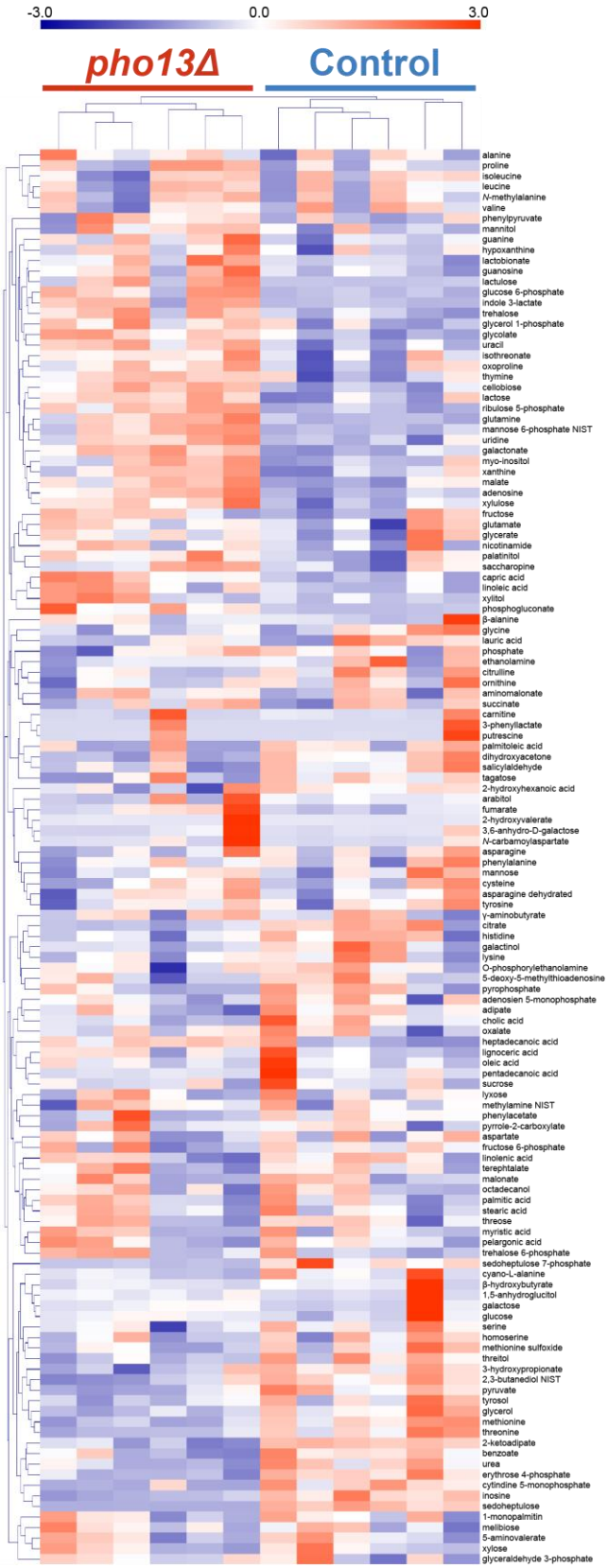

Figure 2.9. Clustered heat map of HCA for metabolomic profiles of SR7 and SR7 *pho13Δ*.

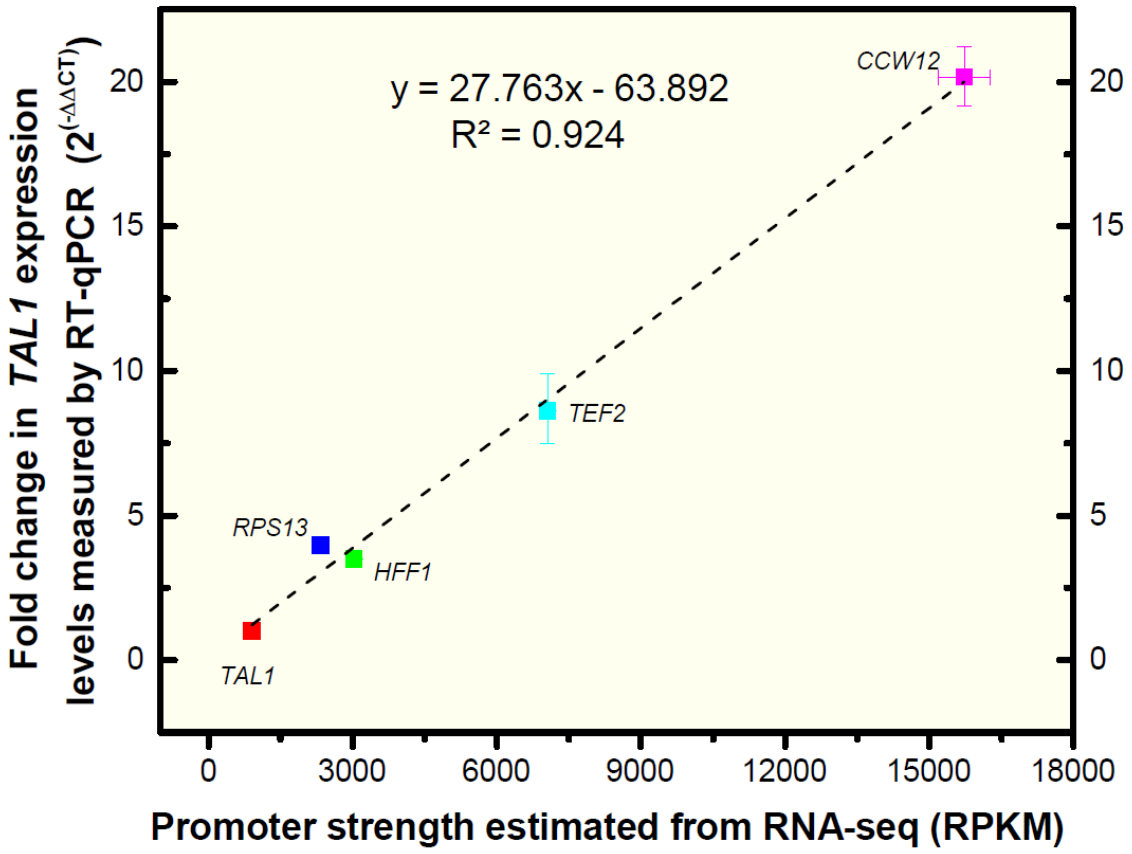

Figure 2.10. Linear correlation between theoretical promoter strength (relative to transcript abundance of the corresponding gene measured by RNA sequencing) and the empirical values (transcript abundance of the engineered *TAL1* gene measured by RT-qPCR). RT-qPCR was performed with both biological and experimental triplicates; the error bars indicate the standard deviations.

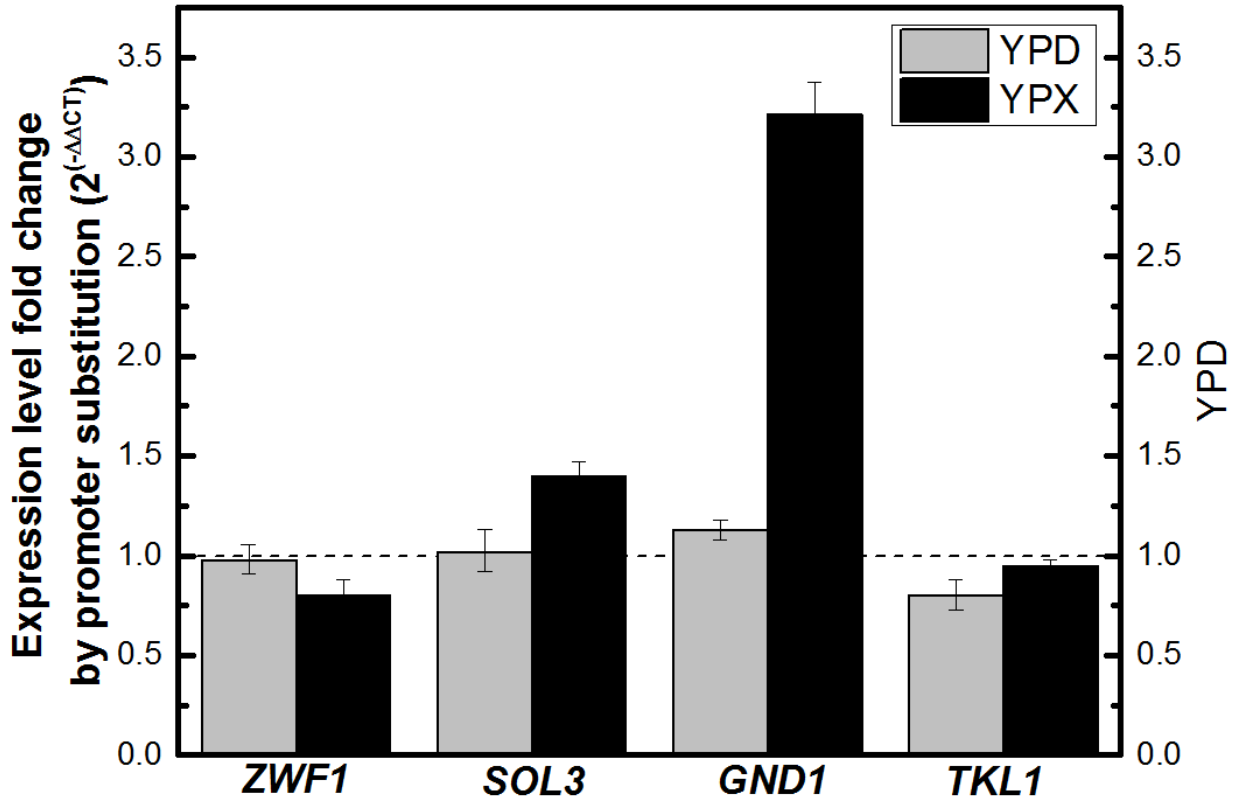

Figure 2.11. Fold changes of PP pathway genes expression levels in the SR7 *CCW12p-TAL1* compared with SR7 in both glucose and xylose condition. The expression levels of the mutants and the control strain were measured by RT-qPCR. Error bars indicate standard deviations of three biological replicates.

CHAPTER 3: ENGINEERING *SACCHAROMYCES CEREVISIAE* TO CO-FERMENT GLUCOSE AND XYLOSE BY MUTANT *GAL2* TRANSPORTERS

The content of this chapter is in preparation for submission. I was the first author of the paper, and Ching-Sung Tsai, Stephan Lane, Soo Rin Kim, and Yong-Su Jin, were co-authors. I performed the research with help from the co-authors, and Dr. Yong-Su Jin and Dr. Soo Rin Kim were the directors of the research.

3.1. Introduction

Lignocellulosic biofuel production is widely believed to be a promising strategy to solve the energy crisis without hurting the food supply compared to biofuel generated from food sources (Stephanopoulos, 2007). *Saccharomyces cerevisiae* has been harnessed by human beings for the ethanol production for a long time. And it is currently being used for the production of ethanol from sugarcane because of its high tolerance to ethanol and fermentation inhibitors (Delgenes et al., 1996; Pereira et al., 2015). However, besides glucose, hydrolysates of lignocellulosic biomass consists of a decent amount of pentose. For example, 30% of the biomass in corn stover is xylose (Kim et al., 2012), which cannot be fermented by *Saccharomyces cerevisiae* naturally. In order to achieve xylose utilization in *Saccharomyces cerevisiae*, heterologous xylose pathway from *Scheffersomyces stipitis*, including xylose reductase (XR) and xylitol dehydrogenase (XDH), were introduced into *Saccharomyces cerevisiae* (Kotter and Ciriacy, 1993; Takuma et al., 1991; Tantirungkij et al., 1993). However, XR prefers NADPH to NADH while XDH only can use NAD^+ as a cofactor. Therefore, this will cause severe co-factor imbalance for xylose fermentation, leading to lower ethanol yield (Kim et al., 2013b; Rizzi et al., 1989; Verduyn et al., 1985). To bypass the redox-imbalance problem of the oxido-reductase pathway, people introduced xylose isomerase pathway from different sources into *Saccharomyces cerevisiae* (Brat et al., 2009; Kim et al., 2013b; Lee et al., 2014b; Vilela Lde et al., 2015; Young et al., 2014).

Though engineered *Saccharomyces cerevisiae* is capable of fermenting glucose and xylose separately, the simultaneous co-utilization of glucose and xylose, which shows advantage in terms of higher ethanol yield and titer (Lynd et al., 2008), cannot be achieved yet. The major

hurdle for simultaneous co-fermentation of glucose and xylose is glucose repression, which can be dissected into glucose repression on xylose metabolism (Santangelo, 2006; Subtil and Boles, 2012; Verstrepen et al., 2004) and glucose competitive inhibition on xylose transport (Farwick et al., 2014; Lee et al., 2002; Nijland et al., 2014; Young et al., 2014). Between them, transport inhibition was believed to be the more prominent problem (Subtil and Boles, 2012). Both heterologous sugar transporters, such as Gxf1 from *Candida intermedia* and Sut1 from *Scheffersomyces stipites*, and endogenous sugar transporters had been studied to enable co-fermentation of glucose and xylose (Fonseca et al., 2011; Goncalves et al., 2014; Katahira et al., 2008; Sedlak and Ho, 2004; Young et al., 2012). However, most of these transporters showed preference towards glucose over xylose. Consequently, many groups have tried to engineer a xylose specific transporter by both evolutionary engineering and rational approaches to achieve co-fermentation of glucose and xylose (Farwick et al., 2014; Nijland et al., 2014; Reznicek et al., 2015; Young et al., 2011; Young et al., 2014). Young and his colleagues tried to wire the transporters' preference by programming an identified sequence motif, G-G/F-XXX-G, which is common in most endogenous sugar transporters and heterologous sugar transporter (Young et al., 2014). Their engineered transporters, including mutant *Candida intermedia* gxs1 *Scheffersomyces stipitis* rgt2 and *Saccharomyces cerevisiae* hxt7, enabled transporters-null *Saccharomyces cerevisiae* to grow on xylose but not on glucose. Another study down by Farwick and his colleagues discovered two conserved residues in *Saccharomyces cerevisiae* glucose transporters where mutation of these two residues altered the transporters' preference on glucose and xylose.(Farwick et al., 2014). Among those mutant transporters, they claimed that Gal2-N376F was able to transport xylose without inhibition by glucose, and Gal2-N376V showed relative weak inhibition by glucose (Farwick et al., 2014). However, neither of these two

studies demonstrated fast glucose and xylose co-fermentation by using their mutant transporters. One possible reason is that highly engineered transporters-null strains are not robust. Interestingly, one recent study showed that a widely used transporters-null *Saccharomyces cerevisiae* by LoxP/Cre system suffered from gene losses and chromosomal rearrangement (Solis-Escalante et al., 2015).

Using a CRISPR/Cas9 based multiple-gene deletion technique, *HXT1-7* and *GAL2* were deleted in an engineered *Saccharomyces cerevisiae* strain with an efficient xylose metabolism pathway. The resulting strain could not grow on both glucose and xylose while, by complementation with sugar transporters, the strain retained efficient xylose and glucose fermentation ability. This is the first study showing the benefit of the Cas9 technique for rapid construction of sugar transport deficient *Saccharomyces cerevisiae* strain. Furthermore, by introducing previous reported *GAL2* (Farwick et al., 2014) mutants into our sugar-transport-deficient strain, we are able to achieve fast xylose and glucose co-fermentation.

3.2. Materials and methods

3.2.1. Strains and culture conditions

All strains and plasmids used in this study were listed in Table 3.2. For testing sugar deleted strains (Fig. 3.2 and Fig. 3.7), yeast strains were pre-culture in 5 mL of YP medium (10 g/L yeast extract, 20 g/L Bacto peptone) containing 2% ethanol aerobically at 30°C for 48 hours. For yeast strain harboring pRS41K serial plasmids (Fig. 3.2-3.6 and Fig. 3.8-3.9), yeast strains were pre-culture in 5 mL of YP medium (10 g/L yeast extract, 20 g/L Bacto peptone) containing 40g/L xylose and 200 μg/ml Geneticin aerobically at 30°C for 24 hours. Then cells were harvested and washed twice with sterile water. For fermentation experiments, the initial cell

densities were adjusted to around OD = 1 (optical density at 600nm), which is about 0.47 g/L dry cell weight. Fermentation experiments were conducted under the oxygen-limited condition in 125 mL flasks containing 25 mL medium at 30°C and 100 rpm.

3.2.2. Plasmids and strains construction

To construct pRS41K-*TEF1*$_P$-*GAL2*-*CYC1*$_T$ plasmid, pRS41K--*TEF1*$_P$- *CYC1*$_T$ was linearized with XmaI and EcoRV. Then the *GAL2* gene was PCR from the CEN.PK genome with XmaI and EcoRV digestion site on each side. Next, the *GAL2* gene fragment was digested with XmaI and EcoRV and then ligated with digested pRS41K-*TEF1*$_P$-*CYC1*$_T$ vector.

For cloning pRS41K-*TEF1*$_P$-*GAL2*-*F*-*CYC1*$_T$, pRS41K-*TEF1*$_P$-*GAL2*-*F*-*CYC1*$_T$, and single gRNA vectors, the Fast Cloning method (Li et al., 2011) was applied by using divergent overlapping primers (Table 3.3).

To corporate multiple guide RNA cassettes into one plasmid, in vivo DNA assembler method was used with the help of yeast homologous recombination machinery according to the literature (Shao et al., 2009). After the colony PCR confirmation, desired colonies were cultured, and plasmids were extracted by using yeast plasmid extraction kit (Zymo Research, Irvine, CA). Then plasmids were re-transformed to *E. coli* for later enrichment.

CRISPR/Cas9 guided deletions were performed according to previous literature (Zhang et al., 2014) with some modifications. For the deletion of four genes together, for example, 3 µg gRNA plasmid and 5 µg of each of four donors were added for each transformation.

3.2.3. HPLC analysis

Xylose and glucose concentrations during the fermentation were quantified by high-performance liquid chromatography (HPLC) (Agilent, Santa Clara, CA) with the Rezex RCM-

Monosaccharide Ca+2 (8%) column (Phenomenex Inc., Torrance, CA). Glycerol, xylitol, acetate, and ethanol concentrations were quantified by HPLC with the Rezex ROA-Organic Acid H+ (8%) column (Phenomenex Inc., Torrance, CA). Samples were centrifuged first and the supernatant was used for analyzing.

3.3. Results

3.3.1. Construction and characterization of the sugar-transport-deficient *Saccharomyces cerevisiae* strain

To test the sugar transporters' ability to co-utilize glucose and xylose, a robust xylose-fermenting *Saccharomyces cerevisiae* strain with major sugar transporters deletion is a prerequisite. *HXT1-7* and *GAL2* were deleted in a fast xylose-fermenting strain SR8 (Kim et al., 2013c) by using the CRISPR/Cas9 guided multiple-gene deletion technique. The diagram for constructions of gRNA and deletion mutants were shown in Figure 3.1. For using the CRISPR/Cas9 technique to delete multiple genes at the same time, multiple guide RNA cassettes were cloned into one pRS42H or pRS42K vector by using yeast homologous recombination (Fig. 3.1A). First *HXT1-4* were completely deleted in xylose-fermenting *Saccharomyces cerevisiae* strain SR8, and then *HXT5-7* were deleted. Finally, *GAL2* was deleted. By doing this, a mutant SR8D8 with no glucose or xylose transportation ability was successfully constructed (Fig. 3.1C).

The volumetric glucose consumption rate at 6 hour and the volumetric xylose consumption rate at 24 hour of parental strain SR8, SR8 *HXT1-4*Δ, SR8 *HXT5-7*Δ, SR8 *HXT1-7*Δ and SR8D8 (SR8 *HXT1-7*Δ *GAL2*Δ) were compared (Fig. 3.2A and 3.2B). After deletion of *HXT1-4* or deletion of *HXT5-7*, strains still maintained xylose and glucose fermentation abilities

to a certain extent, while deletion of *HXT1-7* almost reduced glucose and xylose consumption rate to zero. The growth of the parental strain SR8 (Fig. 3.2C) and the growth of SR8D8 (Fig. 3.2D) strain in glucose, xylose, galactose and no sugar conditions were compared. The growth test clearly showed that SR8D8 grew at the same rate in xylose, glucose and galactose conditions as compared to no sugar condition.

3.3.2. Restoration of xylose and glucose fermentation ability by introducing Gal2 transporter

To demonstrate that SR8D8 is an excellent platform strain for studying transporters, a Gal2 transporter was re-introduced into the SR8D8 strain by pRS41K plasmid with the *TEF1* promoter. After that, the strain retained its glucose and xylose consumption ability (Fig. 3.3A and 3B). Previously the deletion mutant, SR8 *HXT1-7*Δ, which still had Gal2 transporter, could not grow in glucose condition. That was because of the glucose repression on GAL genes (Johnston et al., 1994; Lamphier and Ptashne, 1992). But, in this case, the constitutive promoter was used to express Gal2. Then in the mixture of 40 g/L xylose and 40g/L glucose, we could observe the sequential fermentation of glucose and xylose (Fig. 3.3C), which was typical for endogenous hexose transporters. The restoration of xylose and glucose fermentation abilities by introducing endogenous transporter proved the SR8D8's potential for transporter study, especially for testing transporters for the co-fermentation of glucose and xylose.

3.3.3. Overexpression of Gal2-N376V in SR8D8 and the co-fermentation of glucose and xylose by SR8D8 41K-GAL2-V

To achieve co-fermentation of glucose and xylose, a previously reported mutant Gal2 transporter, Gal2-N376V (Young et al., 2014) with relatively weak inhibition from glucose, was overexpressed in SR8D8 by single copy plasmid with geneticin resistance. The resulting strain SR8D8 41K-GAL2-V retained efficient glucose and xylose fermentation abilities (Fig. 3.4A and 4B). Then the mutant was tested for co-fermentation of glucose and xylose in 40 g/L xylose and 40 g/L glucose mixture (Fig. 3.4C). Started with initial OD 1, the mutant was able to consume all the sugar within 36 hours under oxygen limited condition. Both sugars were consumed simultaneously though glucose was consumed faster than xylose. Comparison of SR8D8 41K-GAL2-V and SR8D8 41K-GAL2 in 40 g/L xylose and 40 g/L glucose mixture showed that the mutant Gal2 transporter significantly reduced the lag phase of xylose consumption so that the total fermentation time was reduced, compared with the wild-type Gal2 transporter (Fig. 3.8). The co-fermentation was also achieved under industrially relevant condition with 70g/L glucose and 40g/L xylose (Fig. 3.4D). This result demonstrated the potential of using the Gal2-N376V transporter for co-fermentation in different ratios of glucose and xylose.

3.3.4. Overexpression of Gal2-N376F in SR8D8 and the co-fermentation of glucose and xylose by the co-culture system

It has been reported that mutant Gal2 transporter, Gal2-N376F (Young et al., 2014) could not support growth on glucose, and the xylose transport by this transporter would not be inhibited by glucose. To characterize this transporter, we overexpressed it in SR8D8 by single copy plasmid with geneticin resistance cassette. The resulting strain SR8D8 41K-GAL2-F could

consume glucose and grow in 40g/L glucose with initial OD 1 (Fig. 3.5A) indeed. But the glucose consumption rate was so slow that the generated ethanol was also used during the fermentation. More detailed examination showed that under lower concentrations of sugar with initial OD 0.1, the mutant could barely consume glucose (Fig. 3.9A and B). Then the mutant was also tested in 40g/L pure xylose, and a mixture of 40 g/L glucose and 40 g/L xylose (Fig. 3.5B and 3.5C). In the pure xylose condition, 40 g/L xylose was almost finished within 36 hours while, with the presence of glucose, the mutant took around 48 hours to finish all the xylose. Also, we could observe glucose reduction after 24 hours in the mixture of glucose and xylose. This result suggests that Gal2-N376F indeed can very slowly transport glucose, and the inhibition of glucose to xylose is present, but very weak.

Since Gal2-N376F has very strong preference for xylose, we designed a co-culture system to use both SR8D8 41K-GAL2-F and D452 41K, which could consume glucose only (Fig. 3.5D and 3.5E), for the co-fermentation of glucose and xylose. The fermentation was performed with OD 1 inoculum of D452 41K and OD 10 inoculum of SR8D8 41K-GAL2-F, considering the relatively faster glucose fermentation rate. 70 g/L glucose and 40 g/L xylose could be co-consumed in around 22 hours. This result demonstrates the possibility of co-fermentation of glucose and xylose by using the co-culture system.

3.3.5. The combination effect of Gal2-N376F and Gal2-N376V in SR8D8

Since Gal2-N376F transporter prefers xylose to glucose, introduction of this transporter into SR8D8 41K-GAL2-V may further improve the co-fermentation ability of this strain. Gal2-N376F overexpression cassette with *TEF1* promoter and *CYC1* terminator was integrated into the genome of SR8D8 41K-GAL2-V by the CRISPR/Cas9 technique. The resulting strain SR8D8-F

41K-GAL2-V consumed both glucose and xylose much faster in mixture of glucose and xylose, compared with its parental strain SR8D8 41K-GAL2-V (Fig. 3.10), though the growth of these two strains were almost same. We further compared this co-fermenting strain with the original strain SR8 41K, which is a sequential fermenting strain. Both strains consumed 40 g/L glucose and 40 g/L xylose in around 24 hours (Fig. 3.6A and 3.6B). SR8D8-F 41K-GAL2-V and the original strain SR8 41K were next compared in the industrially relevant concentration of glucose and xylose mixture (Fig. 3.6C and 3.6D). The co-fermentation strained not only showed similar ethanol production rate, but also achieved similar yield as compared to the original strain (Table 3.1).

3.4. Discussion

Finding new transporters to bypass the glucose inhibition at transport level is the key to achieve the co-fermentation of glucose and xylose. Hxt-null *Saccharomyces cerevisiae* strain, constructed by the Loxp/Cre system, was widely used for transporter studies, especially for the purpose of finding xylose transporters free from glucose repression (Farwick et al., 2014; Young et al., 2014). However, the deletion of all native transporters by the Loxp/Cre system caused gene loss and chromosome rearrangement. That's probably why the previous study could not present rapid glucose and xylose co-fermentation phenotype, even if they created mutant transporters with less inhibition by glucose. In the current study, we demonstrated the advantages of using the CRISPR/Cas9 based multiple-gene deletion strategy to construct the sugar-transport-deficient *Saccharomyces cerevisiae* strain. Maximally four transporters were deleted at once, showing the efficiency of CRISPR/Cas9 based gene-editing methods. More importantly, CRISPR/Cas9 based gene-editing methods are clear, which will not leave undesired scars in the

genome (Jakociunas et al., 2015; Mans et al., 2015; Ryan and Cate, 2014; Zhang et al., 2014). Interestingly, after deletion of *HXT1-7*, our mutant could not consume glucose and had very long lag time for xylose consumption (Fig. 3.7). After the further deletion of *GAL2*, the mutant (SR8D8) became sugar-transport-deficient, which proved to be a good platform strain for transporter study. Our SR8D8 strain retained robust glucose and xylose fermentation phenotypes as soon as we re-introduce Gal2 transporter. But the strain showed sequential fermentation phenotype, which was a proof of glucose repression at transport level by wild-type endogenous transporters.

In this study, we demonstrated the feasibility of co-fermentation of glucose and xylose by introducing two mutant Gal2 transporters Gal2-N376F and Gal2-N376V. Though this two transporters had been reported before (Farwick et al., 2014), the inability of their platform strain to ferment xylose efficiently restricted the application of these two transporters for co-fermentation of glucose and xylose. Here, by just introducing one transporter Gal2-N376V into our sugar-transport-deficient strain, we could achieve efficient glucose and xylose co-fermentation even in the industrially relevant concentration (Fig. 3.4D). Also, characterization of Gal2-N376F transporter showed that it could transport glucose, but in a very slow rate, which contradicted the claim from Farwick's study that this transporter could not transport glucose (Farwick et al., 2014). Moreover, the 41K-GAL2-F strain presented strong preference for xylose over glucose in the mixture of glucose and xylose (Fig. 3.5C). Wild-type D452-2 strain can only ferment glucose. So by co-culture of these two yeast strains, which possessed opposite sugar selectivity, we achieved co-fermentation of glucose and xylose. Although people have been using the co-culture of *Saccharomyces cerevisiae* and *Scheffersomyces stipites*, or *Escherichia coli* and *Saccharomyces cerevisiae* to produce ethanol from hexose and pentose (Ashoor et al.,

2015; Eiteman et al., 2008; Karagoz and Ozkan, 2014; Taniguchi et al., 1997), this is the first time that the co-fermentation of glucose and xylose is achieved by using two *Saccharomyces cerevisiae* strains. Notably, without a strain capable of selectively consuming xylose even with the presence of glucose, co-fermenting glucose and xylose by co-culturing two *Saccharomyces cerevisiae* strains would not be achievable.

Although many recent studies focused on transporters engineering to co-ferment xylose and glucose, the fermentation time of their co-fermentation strain was much longer than the sequential fermentation by xylose-fermenting *Saccharomyces cerevisiae* strains without transporter engineering (Nijland et al., 2014; Reznicek et al., 2015; Wang et al., 2015). In our study, by the combination of Gal2-N376F and Gal2-N376V transporters, we enabled the co-fermentation of glucose and xylose at a similar rate of the sequential fermentation by the parental strain. Also, the ethanol yields of co-fermentation and sequential fermentation were similar (Table 3.1). We envision that, by increasing and balancing copy numbers of Gal2-N376F and Gal2-N376V transporters, we may able to achieve even faster co-fermentation of glucose and xylose.

Our study proved that a robust xylose-fermenting *Saccharomyces cerevisiae* strain with major hexose transporters deletion was the prerequisite for achieving rapid co-fermentation of glucose and xylose. By introducing mutant endogenous transporters with balanced preferences for xylose and glucose, co-fermentation of glucose and xylose was achieved in industrially relevant sugar concentration.

3.5. Tables

Table 3.1. Comparison of ethanol yield and ethanol productivity during co-fermentation

	40 g/L glucose and 40 g/L xylose		70 g/L glucose and 40 g/L xylose	
Strain	Ethanol Yield (g/g)	Ethanol Productivity (g/L/h)	Ethanol Yield (g/g)	Ethanol Productivity (g/L/h)
SR8 41K	0.380±0.000	1.194±0.009	0.389±0.002	1.788±0.018
SR8D8 41K-GAL2	0.351±0.003	0.765±0.027	-	-
SR8D8 41K-GAL2-V	0.356±0.000	0.844±0.001	0.361±0.022	1.115±0.059
SR8D8-F 41K-GAL2-V	0.378±0.004	1.217±0.018	0.376±0.001	1.584±0.001

3.6. Figures

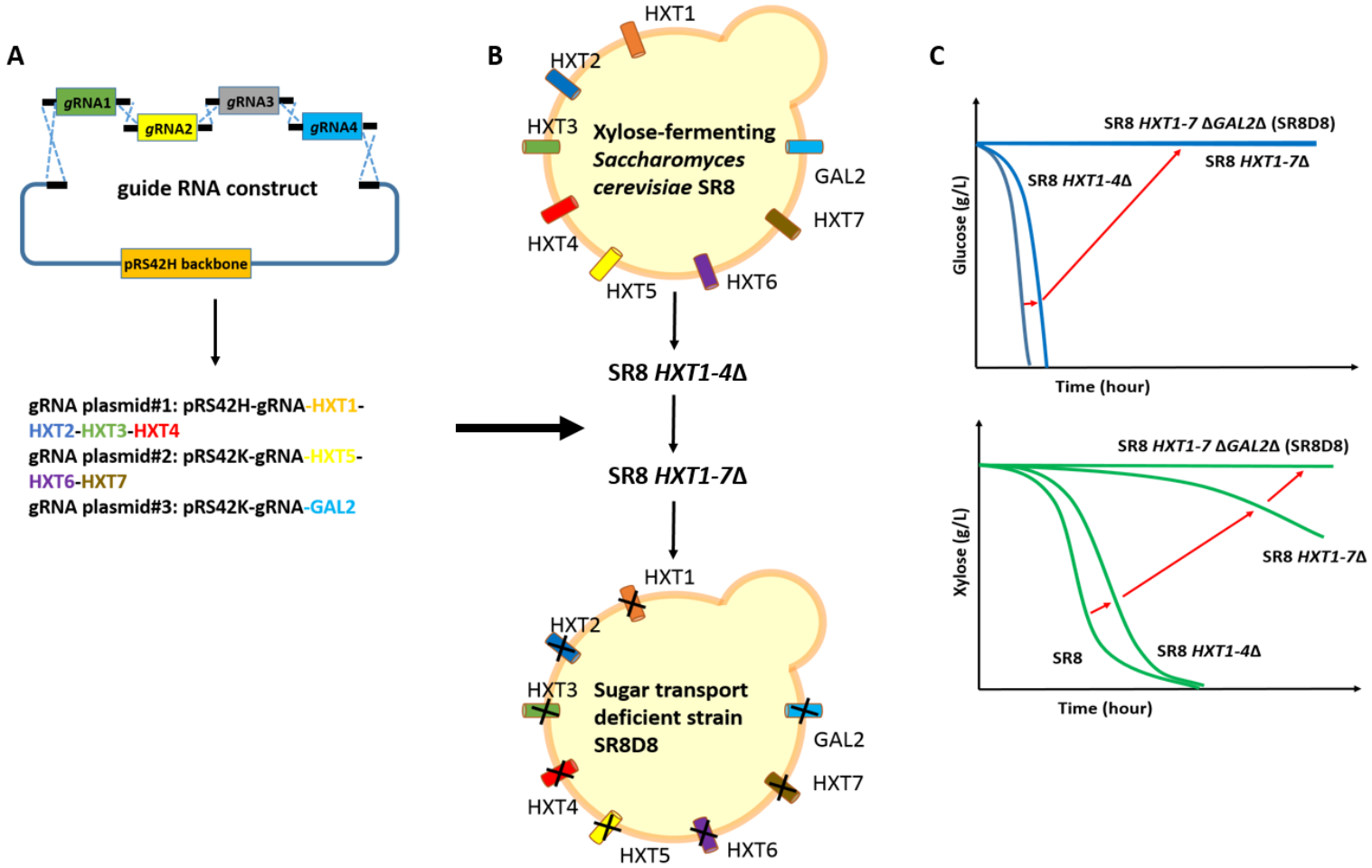

Figure 3.1. Diagram of the sugar-transport-deficient strain construction. (A) Plasmids harboring multiple guide RNA were constructed by homologous recombination. (B) Sequential deletion of *HXT1-7* and *GAL2* by the CRISPR/Cas9 technique. (C) Arbitrary illustration of sugar transport reduction by transporters deletion.

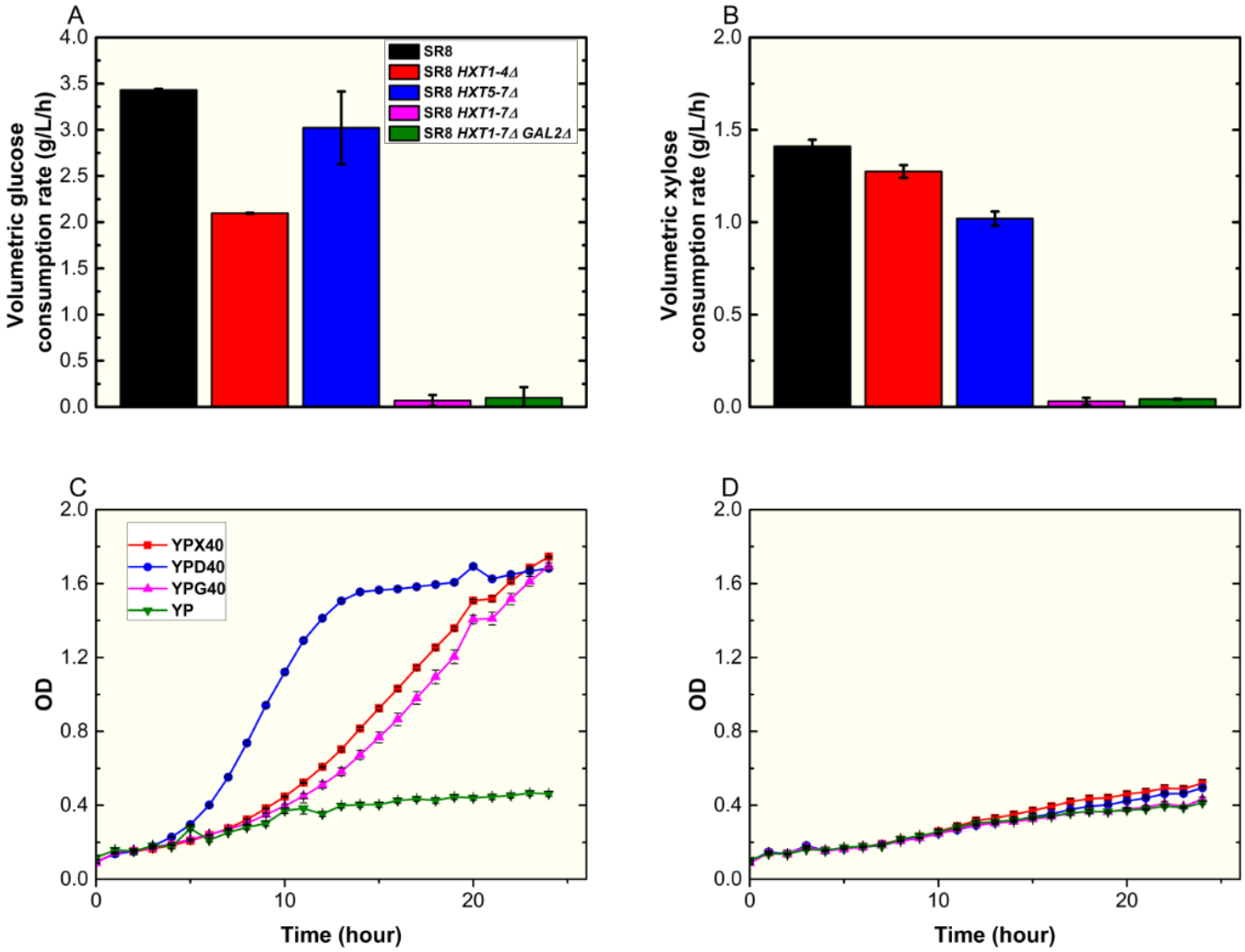

Figure 3.2. Characterization of transporters deletion mutants. (A) Volumetric glucose and (B) volumetric xylose consumption rates of transporters deletion mutants and control strain (SR8) were calculated at 6 hours and 24 hours respectively. Growth of (C) control

strain (SR8) and (D) the sugar-transport-deficient mutant (SR8D8) in complex medium with 40g/L glucose, 40g/L xylose, 40 g/L galactose and no sugar control were monitored. The results are the means of duplicate experiments; the error bars indicate standard deviations.

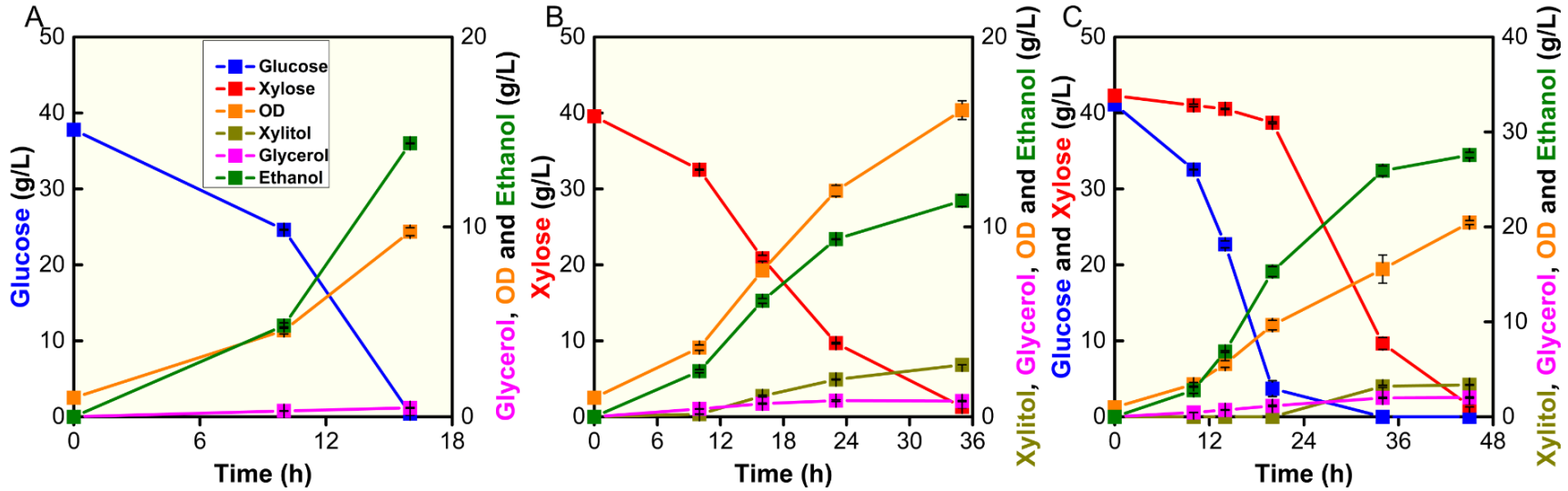

Fig. 3.3. Restoration of sugar transport ability by introducing the Gal2 transporter in the sugar-transport-deficient mutant (SR8D8). Fermentation profiles of strain SR8D8 41K-GAL2 in (A) 40g/L Glucose, (B) 40g/L xylose and (C) the mixture of 40g/L glucose and 40g/L xylose were monitored. The results are the means of duplicate experiments; the error bars indicate standard deviations.

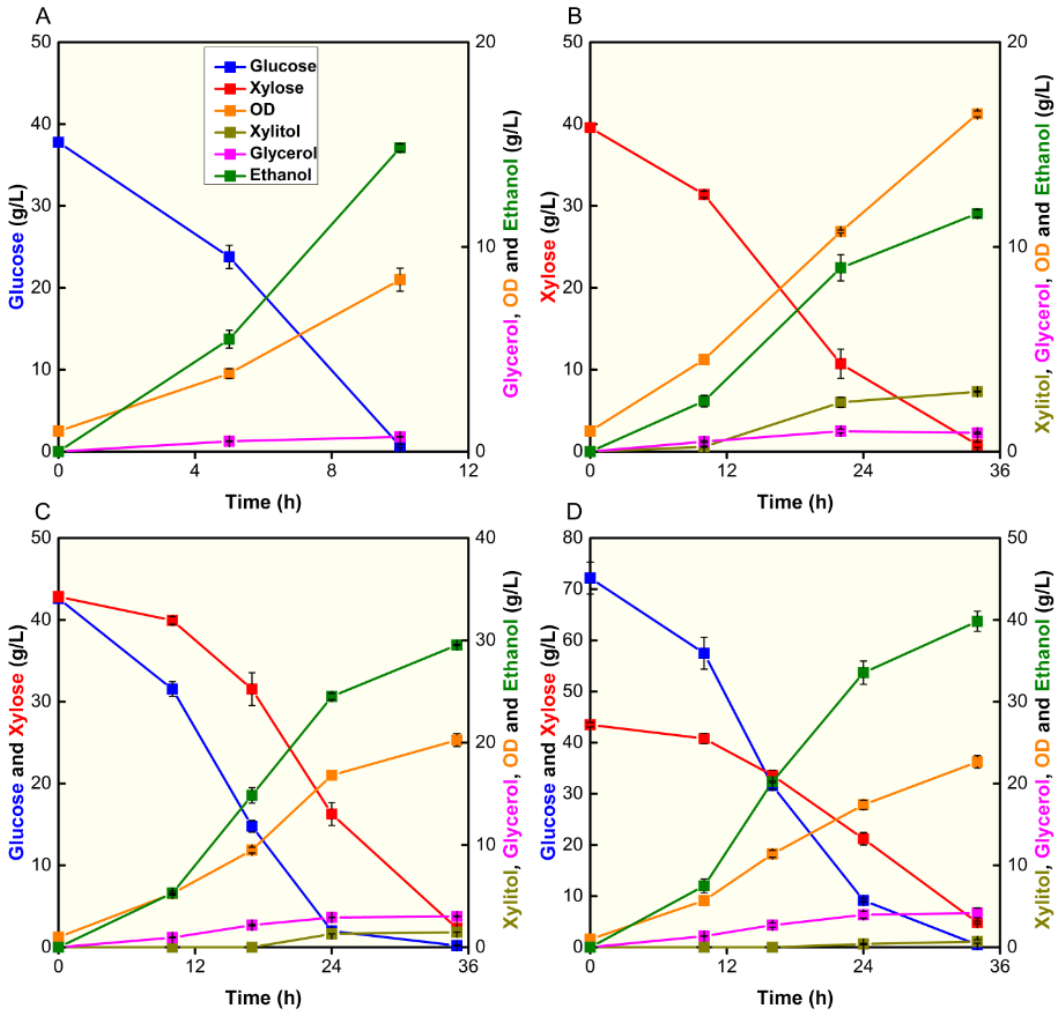

Fig. 3.4. Characterization of the Gal2-N376V transporter. Fermentation profiles of strain SR8D8 41K-GAL2-V in (A) 40g/L Glucose, (B) 40g/L xylose, (C) the mixture of 40g/L glucose and 40g/L xylose, and (D) the mixture of 70g/L glucose and 40 g/L xylose were monitored. The results are the means of duplicate experiments; the error bars indicate standard deviations.

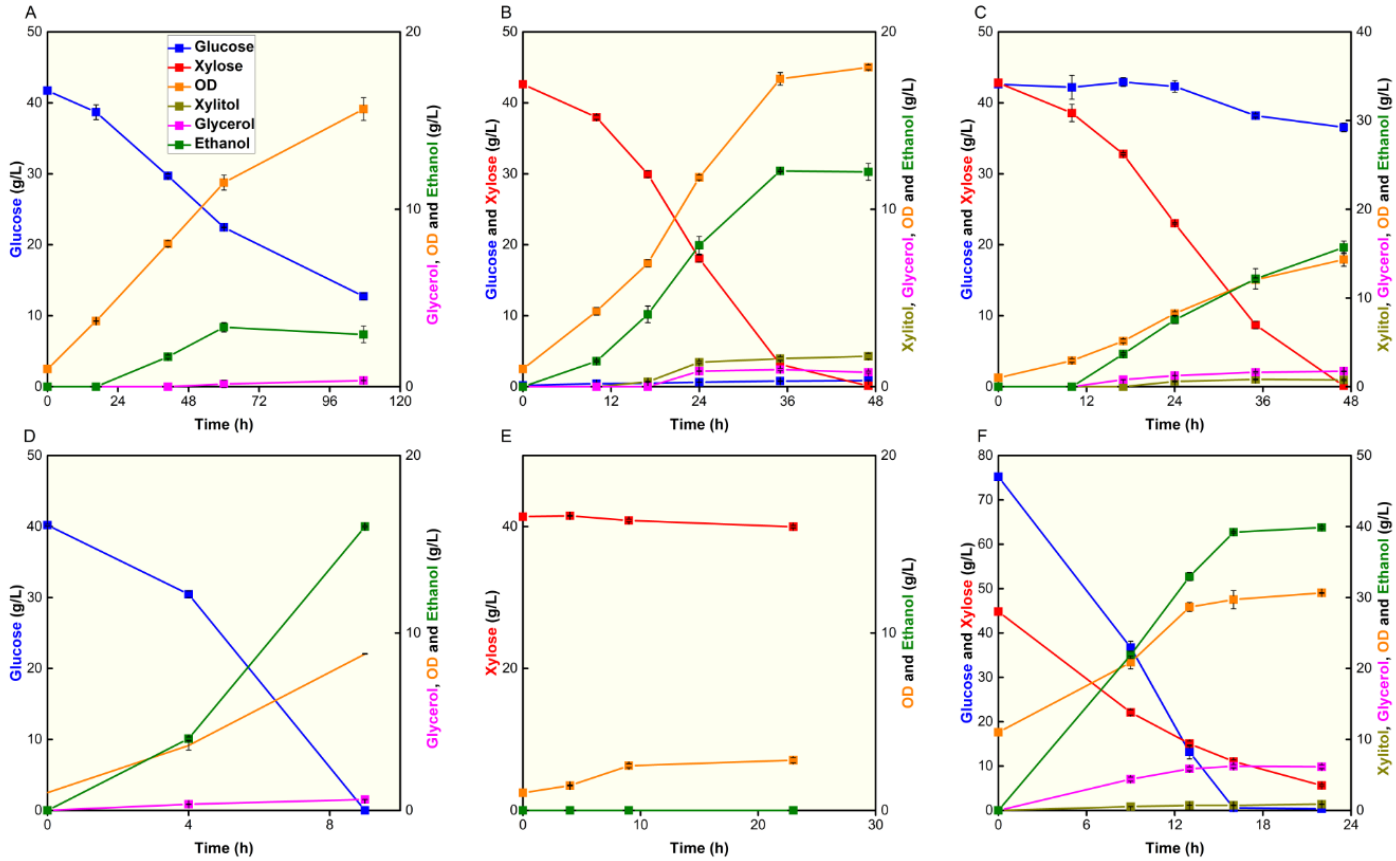

Fig. 3.5. Characterization of the Gal2-N376F transporter and co-fermentation by co-culture system. Fermentation profiles of strain SR8D8 41K-GAL2-F in (A) 40g/L Glucose, (B) 40g/L xylose, and (C) the mixture of 40g/L glucose and 40g/L xylose were monitored. Fermentation profiles of strain D452-2 41K in (D) 40g/L Glucose and (E) 40g/L xylose were monitored. (E) Fermentation profile of the mixture of D452-2 41K with OD 1 and SR8D8 41K-GAL2-F with OD 10 in 70g/L glucose and 40 g/L xylose were monitored. The results are the means of duplicate experiments; the error bars indicate standard deviations.

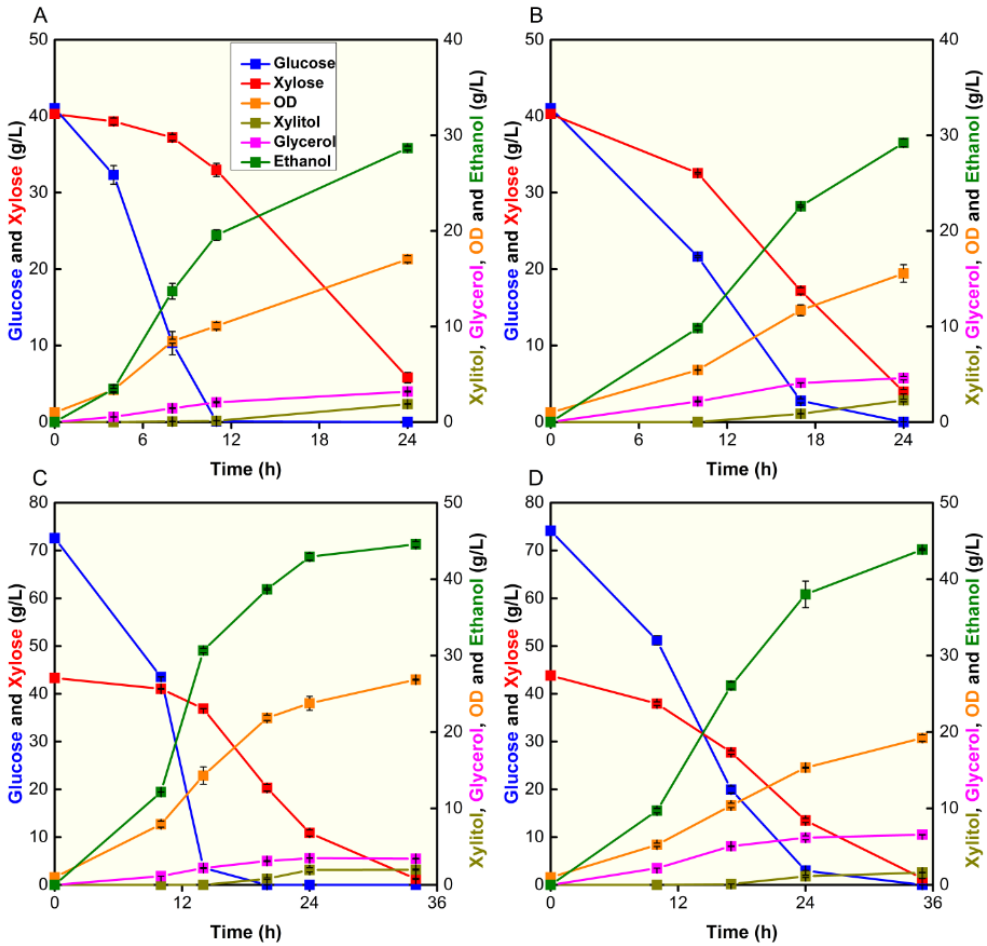

Fig. 3.6. Comparison of SR8D8-F 41K-GAL2-V with control strain (SR8 41K). Fermentation profiles of (A) SR8 41K and (B) SR8D8-F 41K-GAL2-F in the mixture of 40g/L Glucose and 40g/L xylose were compared. Fermentation profiles of (C) SR8 41K and (D) SR8D8-F 41K-GAL2-F in the mixture of 70g/L Glucose and 40g/L xylose were compared. The results are the means of duplicate experiments; the error bars indicate standard deviations.

3.7. Supplementary materials

Table 3.2. List of plasmids and strains used in the study

Plasmid or Strain	Description	Reference
Plasmids		
pRS41N-Cas9	A single-copy plasmid containing Cas9 and a natMX marker	(Zhang et al., 2014)
pRS42H	A multi-copy plasmid containing a Hygromycin B marker	UROSCARF
pRS42H-gRNA-*HXT1* (pCST161)	A multi-copy plasmid containing a guide RNA for *HXT1* deletion and a Hygromycin B marker	This study
pRS42H-gRNA-*HXT2* (pCST162)	A multi-copy plasmid containing a guide RNA for *HXT2* and a Hygromycin B marker	This study
pRS42H-gRNA-*HXT3* (pCST163)	A multi-copy plasmid containing a guide RNA for *HXT3* and a Hygromycin B marker	This study
pRS42H-gRNA-*HXT4* (pCST164)	A multi-copy plasmid containing a guide RNA for *HXT4* and a Hygromycin B marker	This study
pRS42H-gRNA-*HXT5* (pCST165)	A multi-copy plasmid containing a guide RNA for *HXT5* and a Hygromycin B marker	This study
pRS42H-gRNA-*HXT6* (pCST166)	A multi-copy plasmid containing a guide RNA for *HXT6* and a Hygromycin B marker	This study
pRS42H-gRNA-*HXT7* (pCST167)	A multi-copy plasmid containing a guide RNA for *HXT7* and a Hygromycin B marker	This study
pRS42K-gRNA-*GAL2*	A multi-copy plasmid containing a guide RNA a for *GAL2* and a Geneticin marker	This study
pRS42H-gRNA-*HXT1-4*	A multi-copy plasmid containing four guide RNA and a Hygromycin B marker	This study
pRS42H-gRNA-Int	A multi-copy plasmid containing a guide RNA for integration and a Hygromycin B marker	This study
pRS42K-gRNA-*HXT5-7*	A multi-copy plasmid containing three guide RNA and a Geneticin marker	This study
pRS41K	A single-copy plasmid containing a Geneticin marker	UROSCARF
pRS41K-$TEF1_P$-$CYC1_T$	A single-copy plasmid containing a Geneticin marker and *TEF1* promoter and *CYC1* terminator	This study
pRS41K-$TEF1_P$-*GAL2*-$CYC1_T$	*GAL2* under the control of *TEF1* promoter in pRS41K	This study
pRS41K-$TEF1_P$-*GAL2-F*-$CYC1_T$	*GAL2-N376F* under the control of *TEF1* promoter in pRS41K	This study
pRS41K-$TEF1_P$-*GAL2-V*-$CYC1_T$	*GAL2-N376F* under the control of *TEF1* promoter in pRS41K	This study
Strains		
SR8	*S. cerevisiae* D452-2 with a xylose pathway (*S. stipitis XYL1*, *XYL2*, and *XYL3*), *PHO13*Δ, *ALD6*Δ	(Kim et al., 2013c)
SR8 pRS41N-Cas9	SR8 with Cas9 protein expressing plasmid	This study

SR8 41K	SR8 with pRS41K empty vector	This study
SR8 *HXT1-4*Δ	SR8 with *HXT1-4* deletion	This study
SR8 *HXT5-7*Δ	SR8 with *HXT5-4* deletion	This study
SR8 *HXT1-7*Δ	SR8 with *HXT1-7* deletion	This study
SR8 *HXT1-7*Δ*GAL2*Δ (SR8D8)	SR8 with *HXT1-7* and *GAL2* deletion	This study
SR8D8 41K-GAL2	SR8D8 with pRS41K-$TEF1_P$-*GAL2*-$CYC1_T$	This study
SR8D8 41K-GAL2-F	SR8D8 with pRS41K-$TEF1_P$-*GAL2-F*-$CYC1_T$	This study
SR8D8 41K-GAL2-V	SR8D8 with pRS41K-$TEF1_P$-*GAL2-V*-$CYC1_T$	This study
SR8D8-F	SR8D8 with *GAL2-N376F* integration	This study
SR8D8-F 41K-GAL2-V	SR8D8-F with pRS41K-$TEF1_P$-*GAL2-V*-$CYC1_T$	This study

Table 3.2 (cont.)

Table 3.3. List of primers used in the study

Name	Sequence (5'→3')	Description
SOO743	GCC CCCGGG AAAA ATGGCAGTTGAGGAGAACAATATG	*GAL2*_for_XmaI
SOO744	GGC GATATC TTATTCTAGCATGGCCTTGTACC	*GAL2*_rev_EcoRV
SOO759	TAGTCTTCTTTGCCTCCACTTTCTTTAG	*GAL2*_N376F_for
SOO760	GCAAAGAAGACTACACCAATGACAATGG	*GAL2*_N376F_rev
SOO761	TAGTCGTCTTTGCCTCCACTTTCTTTAG	*GAL2*_N376V_for
SOO762	GCAAAGACGACTACACCAATGACAATGG	*GAL2*_N376V_rev
Jin3262	TCATGTTCTTTCCCCACCTTAAAATCTATAAAGATATCATAATCGTCAACTAGTTGATATACGTA AAATCCGGTTTCTGTTGGTCGTAGA	*HXT1*_donor_for
Jin3263	CTTTATAAAATTTACTGAGAAATTAAATACTGTATAAGTCATTAAAATATGCATATTGAGCTTGT TTAGTTCTACGACCAACAGAAACCG	*HXT1*_ donor_rev
Jin3266	TCTCAATTCCTCTTATATTAGATTATAAGAACAACAAATTAAATTACAAAAAGACTTATAAAGC AACATACGAGCGACTCGATGATCAAC	*HXT2*_ donor_for
Jin3267	GAAGATCATCTATTAAAGTATTAGTAGCCATTAGCCTTAAAAAAATCAGTGCTAGTTTAAGTAT AATCTCGTTGATCATCGAGTCGCTCG	*HXT2*_ donor_rev
Jin3343	ATAATTTTACTTAATAGCTTTTCATAAATAATAGAATCACAAACAAAATTTACATCTGAGTTAAA CAATCACGATGCTGAAGGCTCAGGT	*HXT3*_ donor_for

Jin3344	TTTATCATTATTGACTAGCACATCGAATCTTAAAATACACTATTATTCAGCACTACGGTTTAGCG TGAAAACCTGAGCCTTCAGCATCGT	*HXT3*_ donor_rev
Jin3347	GAAAAGATATATTCAAAGCCTCTTATCAAGGTTTGGTTTTGAAACACTTTTACAATAAAATCTGC CAAAATCATGCATCGTTCCACTGTG	*HXT4*_ donor_for
Jin3348	GCGTTAAAAATTGAAGATCAAATATTATTTTTATTCCTTGAAGGAAGTCTATATTATTTAATTAA CTGACCACAGTGGAACGATGCATGA	*HXT4*_ donor_rev
Jin3454	ATAGCTTTGTTAAAACCAGCAAAAAATATTATTTTTCTAGAAAAAAGAATATATTAGAGGTAAA GAAAGATTGTACACCTACCGGTCACC	*HXT5*_ donor_for
Jin3455	TAAAATTTGAAATGGTGCAATGCTGAACATTGCAAGTATGCGAAAATAGTTGATCCTACACTAC AAGAGAGGTGACCGGTAGGTGTACAA	*HXT5*_ donor_rev
Jin3458	AGTTTTTTTCCTTTAAACGCTGGAAAAAAAGGAGAAATTATTGGAACTTTGCAGAGAATAGTCC GTAGGCGACTGTCTATCGGCTAGG	*HXT6*&*7*_ donor_for
SOO724	CTGCAGGCAAAATTGGAATATTTGTGAATAACAGTGCGGTCGGTAAACAACTGACTTCTTCCCA CTTTGCGACCTAGCCGATAGACAGTC	*HXT6*&*7*_ donor_rev
Jin3466	ATTATCATCAAGAATAGTAATAGTTAAGTAAACACAAGATTAACATAATAAAAAAAATAATTCT TTCATACTGACCTAGATGCAATGACG	*GAL2*_ donor _for
Jin3467	ATTAAAATGAAGAAAAAACGTCAGTCATGAAAAATTAAGAGAGATGATGGAGCGTCTCACTTC AAACGCACGTCATTGCATCTAGGTCAG	*GAL2*_ donor _rev
SOO587	AACCTCGAGGAGAAGTTTTTTTACCCCTCTCCACAGATC CAGGAAACAGCTATGACCATG	Int1_donor_for
SOO588	TAATTAGGTAGACCGGGTAGATTTTTCCGTAACCTTGGTGTC TGTAAAACGACGGCCAGT	Int1_donor_for
SOO728	AAACTAGGAAGAAATGCTGC	*HXT1*_confirm_for
SOO729	CGACTCGGTTATCTGTTAATG	*HXT1*_confirm_rev
SOO632	GTTGACAGGTCAGTTAAGGCACAG	*HXT2*_confirm_for
SOO633	GTTGATCATCGAGTCGCTCG	*HXT2*_confirm_rev
Jin3345	GCAGACAGCCTTCATCTTCTCG	*HXT3*_confirm_for
Jin3346	ACCTGAGCCTTCAGCATCGT	*HXT3*_confirm_rev
Jin3349	CAAGAAACGCTTGGCCTTCG	*HXT4*_confirm_for
Jin3350	CACAGTGGAACGATGCATGA	*HXT4*_confirm_rev
Jin3456	GTTATGTTAAGGTCTCCGATACG	*HXT5*_confirm_for
Jin3457	GGTGACCGGTAGGTGTACAA	*HXT5*_confirm_rev
Jin3460	GCTTACTCAGACACCAACAC	*HXT6*&7_confirm_for
Jin3461	GACCTAGCCGATAGACAGTC	*HXT6*&7_confirm_rev
Jin3468	CAAGACGACAGTAATATGTCTCC	*GAL2*_confirm_for
Jin3469	CGTCATTGCATCTAGGTCAG	*GAL2*_confirm_rev
SOO595	GTCTGCCGAAATTCTGTG	Int1_confirm_for
SOO598	CGGTCAGAAAGGGAAATG	Int1_confrom_rev
SOO601	TTTGTGGACTGTCGAAAACT GTTTTAGAGCTAGAAATAGCAAGTT	gRNA plasmid *GAL2* Forward
SOO602	AGTTTTCGACAGTCCACAAA GATCATTTATCTTTCACTGCGGAGA	gRNA plasmid *GAL2* Reverse

Table 3.3 (cont.)

CST515	TGTGTTATGGTTGCTTTCGGGTTTTAGAGCTAGAAATAGCAAGTTAAA	pCST161 *HXT1* Forward
CST516	ACCCGAAAGCAACCATAACACAGATCATTTATCTTTCACTGCGGA	pCST161 *HXT1* Reverse
CST517	TGTGTTATGGTTGCTTTCGG	pCST161 Check
CST518	CAAAGCCAATCGCCGCATATGTTTTAGAGCTAGAAATAGCAAGTTAAA	pCST162 *HXT2* Forward
CST519	ACATATGCGGCGATTGGCTTTGGATCATTTATCTTTCACTGCGGA	pCST162 *HXT2* Reverse
CST520	CAAAGCCAATCGCCGCATAT	pCST162 Check
CST521	CCTGCCTTCGAATAGCTCTCGTTTTAGAGCTAGAAATAGCAAGTTAAA	pCST163 *HXT3* Forward
CST522	ACGAGAGCTATTCGAAGGCAGGGATCATTTATCTTTCACTGCGGA	pCST163 *HXT3* Reverse
CST523	CCTGCCTTCGAATAGCTCTC	pCST163 Check
CST524	AATTAGAATCGGATTCAACGTTTTAGAGCTAGAAATAGCAAGTTAAA	pCST164 *HXT4* Forward
CST525	ACGTTGAATCCGATTCTAATTGATCATTTATCTTTCACTGCGGA	pCST164 *HXT4* Reverse
CST526	AATTAGAATCGGATTCAAC	pCST164 Check
CST527	TCAGGAAACTCGACTGCTCCGTTTTAGAGCTAGAAATAGCAAGTTAAA	pCST165 *HXT5* Forward
CST528	ACGGAGCAGTCGAGTTTCCTGAGATCATTTATCTTTCACTGCGGA	pCST165 *HXT5* Reverse
CST529	TCAGGAAACTCGACTGCTCC	pCST165 Check
CST530	CAACTACGACGCTGAAGAAAGTTTTAGAGCTAGAAATAGCAAGTTAAA	pCST166 *HXT6* Forward
CST531	ACTTTCTTCAGCGTCGTAGTTGGATCATTTATCTTTCACTGCGGA	pCST166 *HXT6* Reverse
CST532	CAACTACGACGCTGAAGAAA	pCST166 Check
CST533	GTCGTAGTTGGCACCTCTTCGTTTTAGAGCTAGAAATAGCAAGTTAAA	pCST167 *HXT7* Forward
CST534	ACGAAGAGGTGCCAACTACGACGATCATTTATCTTTCACTGCGGA	pCST167 *HXT7* Reverse
CST535	GTCGTAGTTGGCACCTCTTC	pCST167 Check
CST561	GCCAGAGGTATAGACATAGCCAGACCTACCTAATTGGTGCATCAGGTGGTCATGGCCCTTCCT GTGTGAAATTGTTATCCGC	Primer with linker sequence
CST562	GTGCCTATTGATGATCTGGCGGAATGTCTGCCGTGCCATAGCCATGCCTTCACATATAGTAACG TCGTGACTGGGAAAAC	Primer with linker sequence
CST563	ACTATATGTGAAGGCATGGCTATGGCACGGCAGACATTCCGCCAGATCATCAATAGGCACCAG GAAACAGCTATGAC	Primer with linker sequence
CST564	GTTGAACATTCTTAGGCTGGTCGAATCATTTAGACACGGGCATCGTCCTCTCGAAAGGTGGTAA AACGACGGCCAG	Primer with linker sequence
CST565	CACCTTTCGAGAGGACGATGCCCGTGTCTAAATGATTCGACCAGCCTAAGAATGTTCAACCAG GAAACAGCTATGAC	Primer with linker sequence
CST566	CTAGCGTGTCCTCGCATAGTTCTTAGATTGTCGCTACGGCATATACGATCCGTGAGACGTGTAA AACGACGGCCAG	Primer with linker sequence
CST567	ACGTCTCACGGATCGTATATGCCGTAGCGACAATCTAAGAACTATGCGAGGACACGCTAGCAG GAAACAGCTATGAC	Primer with linker sequence
CST568	AATCACTCTCCATACAGGGTTTCATACATTTCTCCACGGGACCCACAGTCGTAGATGCGTGTAA AACGACGGCCAG	Primer with linker sequence

Table 3.3 (cont.)

CST569	ACGCATCTACGACTGTGGGTCCCGTGGAGAAATGTATGAAACCCTGTATGGAGAGTGATTCAG GAAACAGCTATGAC	Primer with linker sequence
CST572	AAGGGCCATGACCACCTGATGCACCAATTAGGTAGGTCTGGCTATGTCTATACCTCTGGCGTAA AACGACGGCCAG	Primer with linker sequence

Table 3.3 (cont.)

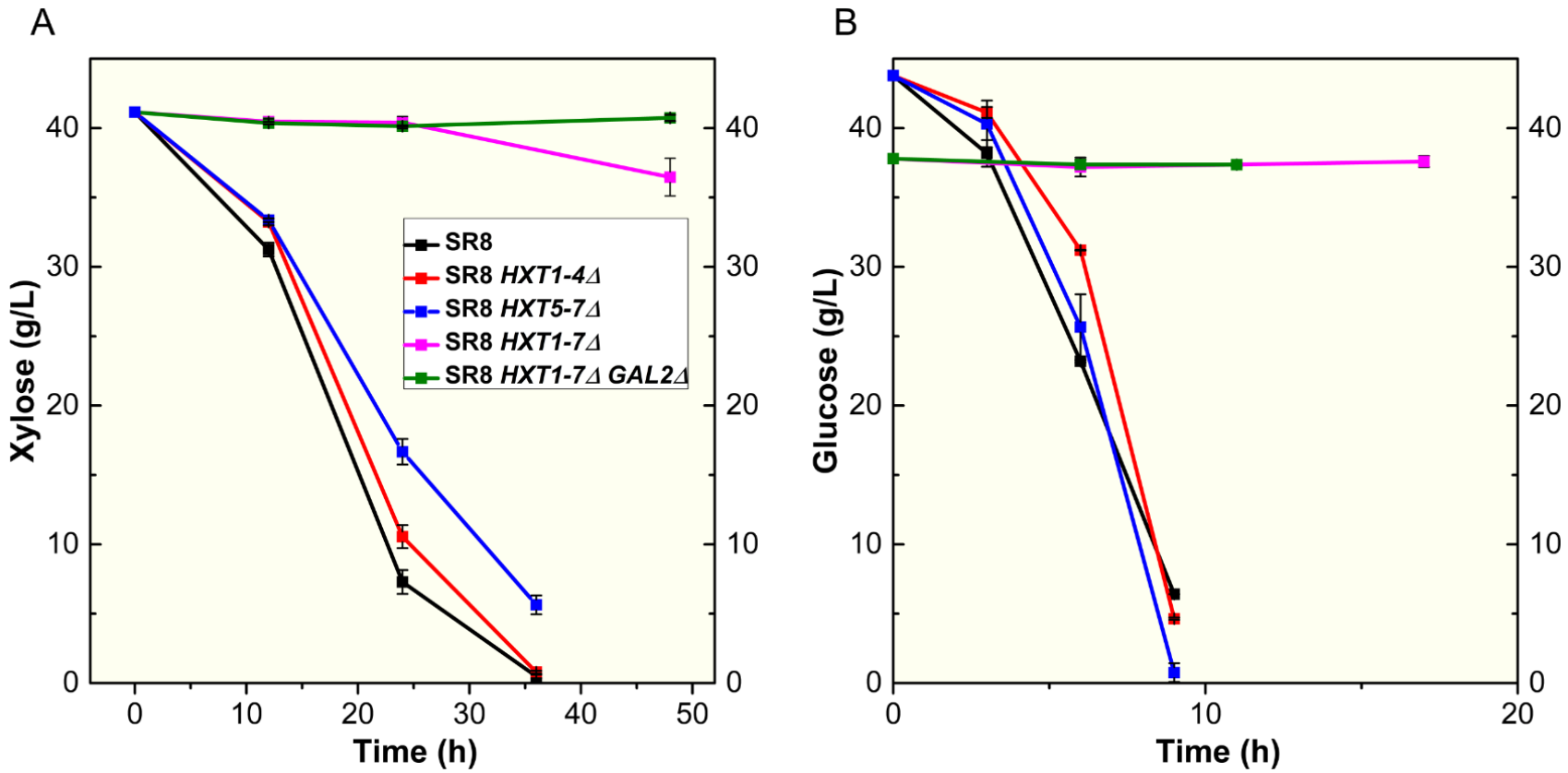

Figure 3.7. (A) Glucose consumption and (B) xylose consumption of transporters deletion mutants and control strain (SR8) were compared. The results are the means of duplicate experiments; the error bars indicate standard deviations.

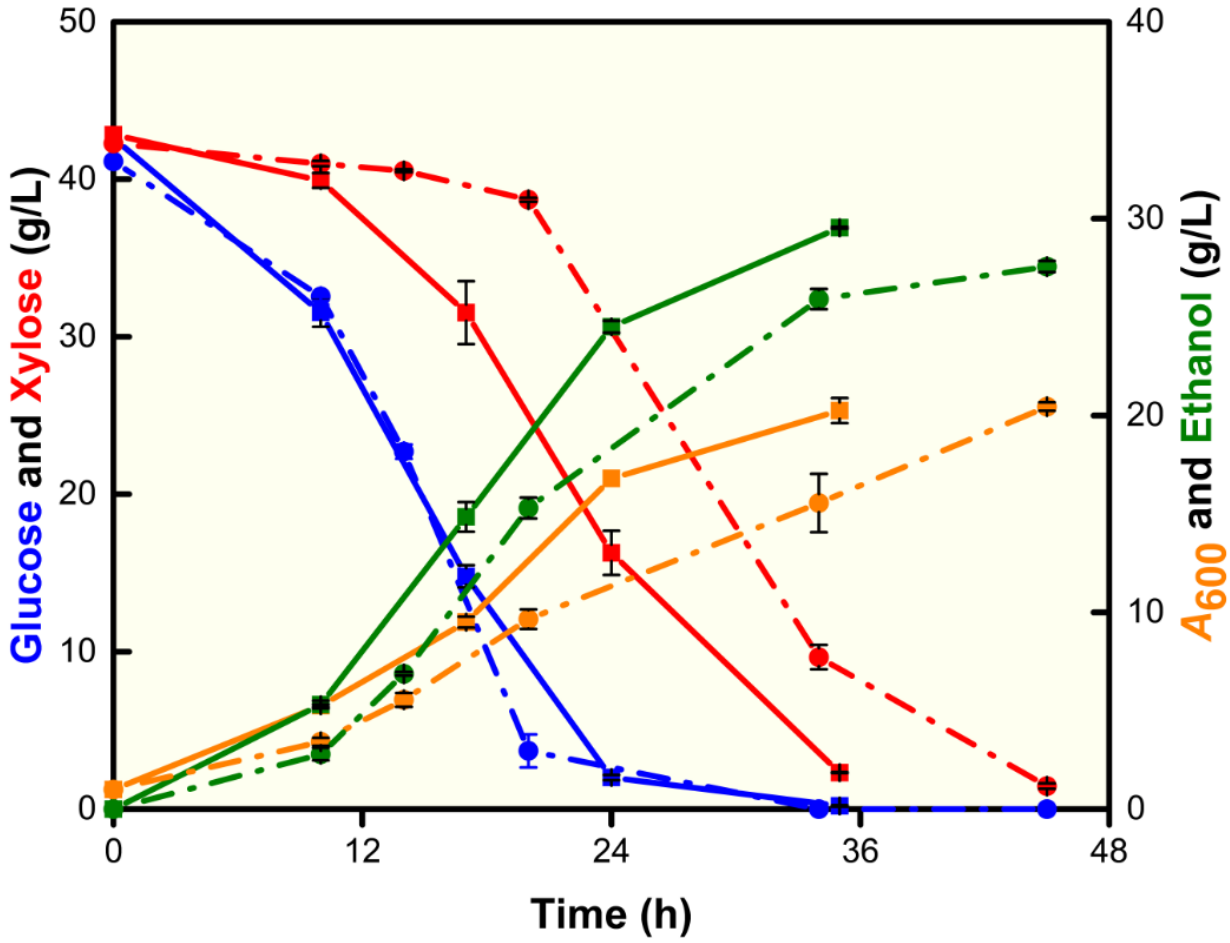

Figure 3.8. Fermentation profiles of SR8D8 41K-GAL2-V (solid line with square) and SR8D8 41K-GAL2 (dash line with circle) in the mixture of 40 g/L glucose and 40 g/L xylose were compared. The results are the means of duplicate experiments; the error bars indicate standard deviations.

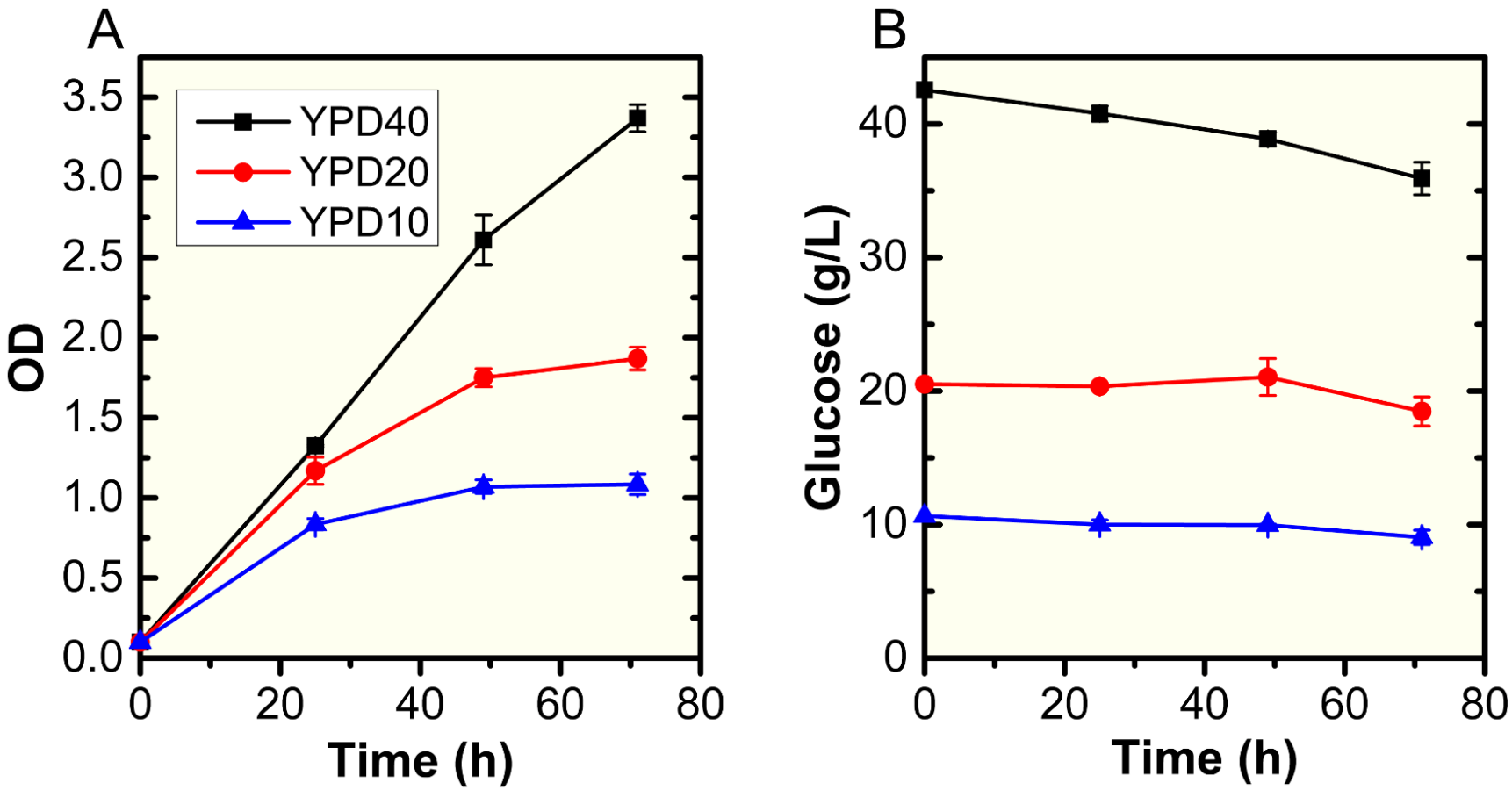

Figure 3.9. (A) Growth and (B) glucose consumption of SR8D8 41K-GAL2-F in different glucose concentrations were compared. The results are the means of duplicate experiments; the error bars indicate standard deviations.

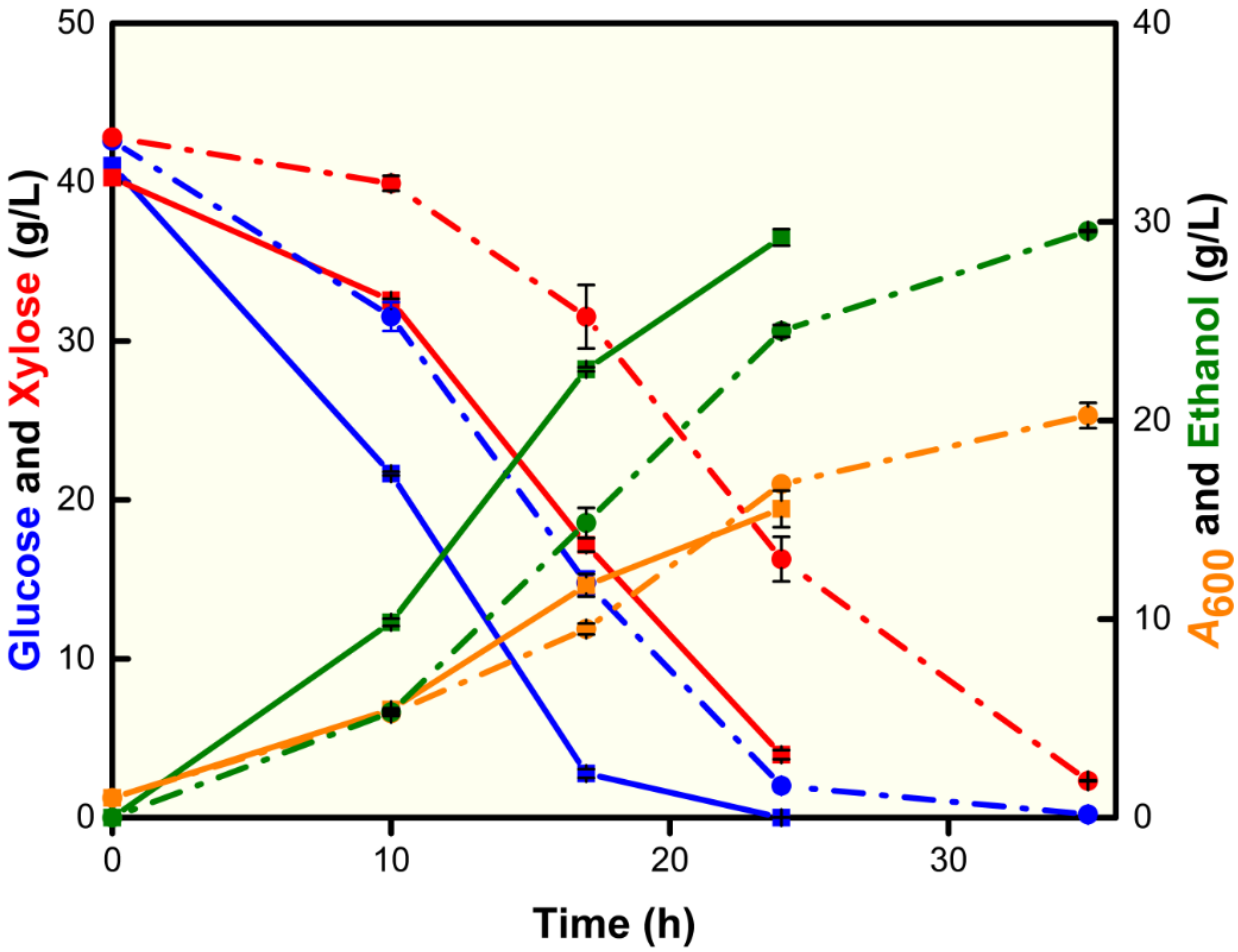

Figure 3.10. Fermentation profiles of SR8D8-F 41K-GAL2-V (solid line with square) and SR8D8 41K-GAL2-V (dash line with circle) in the mixture of 40 g/L glucose and 40 g/L xylose were compared. The results are the means of duplicate experiments; the error bars indicate standard deviations.

CHAPTER 4: CONCLUSIONS AND FUTURE WORK

4.1. Conclusions

4.1.1 Study for improving xylose metabolism

After the introduction of heterologous xylose-assimilating pathway, *Saccharomyces cerevisiae* always suffered from the inefficient xylose metabolism, which could be relieved by *pho13Δ*. Our metabolomics study showed that sedoheptulose and sedoheptulose-7-phophate (S7P) accumulated in the slow xylose-fermenting strain. However, *pho13Δ* significantly reduced the accumulation of these two intermediates. This result revealed the unique metabolic pattern of *Saccharomyces cerevisiae* during xylose fermentation.

S7P is the substrate of transaldolase (Tal1), and our previous study showed that *pho13Δ* could up-regulate the expression of several PP pathway genes, including *TAL1*. Therefore, we used the Cas9-guided promoter substitution technique to modulate *TAL1* expression level. The strengths of promoters for substitution were selected according to the RNA sequencing results of the parental strain. Interestingly, the *TAL1* expression levels of all the mutants strain with the promoter substitution showed a perfect correlation with their theoretical promoter strengths according to the RT-qPCR results. This correlation proved that coupling the Cas9-guided promoter substitution technique with RNA-seq based promoters probing worked efficiently for modulating target gene expression.

Moreover, the phenotypic characterization of these mutants showed that *TAL1* expression was positively correlated with xylose consumption rate but negatively correlated with sedoheptulose and S7P accumulation, which substantiated our hypothesis that *TAL1* up-regulation induced by *pho13Δ* deletion was the primary machinery for reducing sedoheptulose and S7P accumulation and improving xylose metabolism.

Notably, if we modulated *TAL1* expression level to the same level as induced by *pho13Δ*, the resulting strain did not consume xylose as fast as the *pho13Δ* strain. Only when we excessively overexpressed *TAL1*, the resulting strain could consume xylose as fast as the *pho13Δ* strain. This result suggested that there might be other effects caused by *pho13Δ* that contributed to xylose metabolism. Therefore, *GND1*, which was the most up-regulated gene by *pho13Δ*, was overexpressed in slow xylose-fermenting strain. However, we did not observe any significant phenotypic changes with confirmed *GND1* overexpression. This result confirmed that the metabolic change in *pho13Δ* strain was not caused solely by *GND1* up-regulation.

Finally, the catalytic activity of Pho13 was examined, which showed that Pho13 had non-specific phosphatase activity on all PP pathway intermediates including S7P. This result suggested that when S7P is accumulated significantly in the slow xylose-fermenting strain, the non-specific phosphatase, Pho13, might dephosphorylate them to sedoheptulose, which was a dead end molecule inside of the cell. This conversion would cause carbon loss and waste energy so that the strain could not ferment xylose optimally.

4.1.2. Study for the co-fermentation of glucose and xylose

In this study, we constructed a sugar-transport-deficient xylose-fermenting strain by the Cas9-guided multiple-gene deletion technique. *HXT1-7* and *GAL2* were deleted during the process of strain construction. The deletion of *HXT1-4* or *HXT5-7* did not hamper the xylose or glucose transport a lot. But the deletion of *HXT1-7* almost destroyed the transport of both sugars.

The sugar-transport-deficient strain retained efficient xylose and glucose metabolism by the overexpression of the Gal2 transporter, which suggested that the serial deletions of transporters did not cause side effects on the sugar metabolism. In the mixture of glucose and

xylose, the Gal2 overexpression strain showed sequential fermentation phenotype, which was common among wild-type hexose transporters in *Saccharomyces cerevisiae*.

Furthermore, mutant hexose transporter Gal2-N376V or Gal2-N376F was overexpressed in the sugar-transport-deficient strain for characterizations. On one hand, the strain with Gal2-N376V transporter co-fermented glucose and xylose efficiently in different ratios of glucose and xylose. On the other hand, the strain with Gal2-N376V transporter showed strong selectivity towards xylose. Thus, we used this strain and another yeast strain, with strong selectivity towards glucose, to build a co-culture system for the co-fermentation of glucose and xylose.

Finally, we demonstrated the feasibility of co-fermentation of glucose and xylose with a similar rate as sequential fermentation of parental strain by combining Gal2-N376V transporter and Gal2-N376F transporter in our sugar-transport-deficient strain.

4.2. Future work

Since *TAL1* up-regulation could not completely explain the beneficial effects of *pho13Δ* on the xylose metabolism, further study is required to examine factors besides *TAL1* up-regulation that contribute to xylose metabolism by *pho13Δ*, which may provide new gene targets for improving xylose metabolism.

Glyceraldehyde-3-P (G3P) is the substrate for transaldolase, which couples with S7P. However, G3P is also the substrate for Glyceraldehyde-3-phosphate dehydrogenase. So low expression level of *TAL1* means inferiority of PP pathway for competing G3P with glycolysis. It is worthwhile to investigate how *pho13* represses *TAL1* expression in the natural *Saccharomyces cerevisiae*, which may shed some light on the indigenous priority of different metabolic pathways.

We also examined the *GND1* expression levels of our best *TAL1* overexpression mutant and control strain in both glucose and xylose condition. Interestingly we found the *GND1* expression level of our *TAL1* overexpression mutant is as same as the control strain in glucose condition but significantly higher in xylose condition. Since Gnd1 is the enzyme that converts $NADP^+$ to NADPH and the cofactor imbalance problem of xylose metabolism generates surplus $NADP^+$, it is possible that the expression level of GND1 was regulated by the concentration of $NADP^+$. Further study on this topic is also promising.

Apart from major hexose transporters Hxt1-7 and Gal2, there are other cryptic transporters presence in the *Saccharomyces cerevisiae*. It would be safer to delete all the remaining transporters completely to create a real transporters null strain so that there is no risk that these cryptic transporters will be induced by any chance.

Previous studies reported that Gal2 transporter would degrade through ubiquitination when the cells grow on glucose. So ensuing investigation is needed to study the degradation of our mutant Gal2 transporter during the co-fermentation of glucose and xylose and its influence on the co-fermentation.

In order to further improve our co-fermentation strain, modulating and balancing the promoter strengths or copy numbers of those two mutant transporters are required. To achieve perfect simultaneous co-fermentation of glucose and xylose, the ratio of the abundance of those two mutant transporters is critical.

CHAPTER 5: BIBLIOGRAPHY

Ashoor, S., Comitini, F., Ciani, M., 2015. Cell-recycle batch process of *Scheffersomyces stipitis* and *Saccharomyces cerevisiae* co-culture for second generation bioethanol production. Biotechnol Lett. 37**,** 2213-8.

Billard, P., Menart, S., Fleer, R., Bolotinfukuhara, M., 1995. Isolation and characterization of the gene encoding xylose reductase from *Kluyveromyces Lactis*. Gene. 162**,** 93-97.

Brat, D., Boles, E., Wiedemann, B., 2009. Functional expression of a bacterial xylose isomerase in *Saccharomyces cerevisiae*. Appl Environ Microbiol. 75**,** 2304-11.

Ceusters, J., Godts, C., Peshev, D., Vergauwen, R., Dyubankova, N., Lescrinier, E., De Proft, M. P., Van den Ende, W., 2013. Sedoheptulose accumulation under CO2 enrichment in leaves of *Kalanchoe pinnata*: a novel mechanism to enhance C and P homeostasis? J Exp Bot. 64**,** 1497-1507.

Delgenes, J. P., Moletta, R., Navarro, J. M., 1996. Effects of lignocellulose degradation products on ethanol fermentations of glucose and xylose by *Saccharomyces cerevisiae*, *Zymomonas mobilis*, *Pichia stipitis*, and *Candida shehatae*. Enzyme Microb Technol. 19**,** 220-225.

Denkert, C., Budczies, J., Weichert, W., Wohlgemuth, G., Scholz, M., Kind, T., Niesporek, S., Noske, A., Buckendahl, A., Dietel, M., Fiehn, O., 2008. Metabolite profiling of human colon carcinoma--deregulation of TCA cycle and amino acid turnover. Mol Cancer. 7**,** 72.

Diao, L., Liu, Y., Qian, F., Yang, J., Jiang, Y., Yang, S., 2013. Construction of fast xylose-fermenting yeast based on industrial ethanol-producing diploid *Saccharomyces cerevisiae* by rational design and adaptive evolution. BMC Biotechnol. 13**,** 110.

DiCarlo, J. E., Norville, J. E., Mali, P., Rios, X., Aach, J., Church, G. M., 2013. Genome engineering in *Saccharomyces cerevisiae* using CRISPR-Cas systems. Nucleic Acids Res. 41**,** 4336-43.

Dromms, R. A., Styczynski, M. P., 2012. Systematic applications of metabolomics in metabolic engineering. Metabolites. 2**,** 1090-122.

Eiteman, M. A., Lee, S. A., Altman, E., 2008. A co-fermentation strategy to consume sugar mixtures effectively. J Biol Eng. 2**,** 3.

Farwick, A., Bruder, S., Schadeweg, V., Oreb, M., Boles, E., 2014. Engineering of yeast hexose transporters to transport D-xylose without inhibition by D-glucose. Proc Natl Acad Sci U S A. 111**,** 5159-5164.

Fonseca, C., Olofsson, K., Ferreira, C., Runquist, D., Fonseca, L. L., Hahn-Hagerdal, B., Liden, G., 2011. The glucose/xylose facilitator Gxf1 from *Candida intermedia* expressed in a xylose-fermenting industrial strain of *Saccharomyces cerevisiae* increases xylose uptake in SSCF of wheat straw. Enzyme Microb Technol. 48**,** 518-525.

Fujitomi, K., Sanda, T., Hasunuma, T., Kondo, A., 2012. Deletion of the *PHO13* gene in *Saccharomyces cerevisiae* improves ethanol production from lignocellulosic hydrolysate in the presence of acetic and formic acids, and furfural. Bioresource Technol. 111**,** 161-166.

Goncalves, D. L., Matsushika, A., de Sales, B. B., Goshima, T., Bon, E. P., Stambuk, B. U., 2014. Xylose and xylose/glucose co-fermentation by recombinant *Saccharomyces cerevisiae* strains expressing individual hexose transporters. Enzyme Microb Technol. 63**,** 13-20.

Hahn-Hagerdal, B., Karhumaa, K., Jeppsson, M., Gorwa-Grauslund, M. F., 2007. Metabolic engineering for pentose utilization in *Saccharomyces cerevisiae*. Adv Biochem Eng Biotechnol. 108**,** 147-77.

Han, M. J., Lee, J. W., Lee, S. Y., 2011. Understanding and engineering of microbial cells based on proteomics and its conjunction with other omics studies. Proteomics. 11**,** 721-743.

Hasunuma, T., Ismail, K. S., Nambu, Y., Kondo, A., 2014. Co-expression of *TAL1* and *ADH1* in recombinant xylose-fermenting *Saccharomyces cerevisiae* improves ethanol production from lignocellulosic hydrolysates in the presence of furfural. J Biosci Bioeng. 117**,** 165-9.

Ho, N. W. Y., Chen, Z., Brainard, A. P., 1998. Genetically engineered *Saccharomyces* yeast capable of effective co-fermentation of glucose and xylose. Appl Environ Microbiol. 64**,** 1852-1859.

Jakociunas, T., Bonde, I., Herrgard, M., Harrison, S. J., Kristensen, M., Pedersen, L. E., Jensen, M. K., Keasling, J. D., 2015. Multiplex metabolic pathway engineering using CRISPR/Cas9 in *Saccharomyces cerevisiae*. Metab Eng. 28**,** 213-22.

Jeffries, T. W., Jin, Y. S., 2004. Metabolic engineering for improved fermentation of pentoses by yeasts. Appl Microbiol Biotechnol. 63**,** 495-509.

Johnston, M., Flick, J. S., Pexton, T., 1994. Multiple mechanisms provide rapid and stringent glucose repression of Gal gene expression in *Saccharomyces cerevisiae*. Mol Cell Biol. 14**,** 3834-3841.

Kaneko, Y., Tohe, A., Banno, I., Oshima, Y., 1989. Molecular characterization of a specific para-nitrophenylphosphatase gene, *Pho13,* and its mapping by chromosome fragmentation in *Saccharomyces cerevisiae*. Mol Gen Genet. 220**,** 133-139.

Karagoz, P., Ozkan, M., 2014. Ethanol production from wheat straw by *Saccharomyces cerevisiae* and *Scheffersomyces stipitis* co-culture in batch and continuous system. Bioresource Technol. 158**,** 286-93.

Karhumaa, K., Fromanger, R., Hahn-Hagerdal, B., Gorwa-Grauslund, M. F., 2007a. High activity of xylose reductase and xylitol dehydrogenase improves xylose fermentation by recombinant *Saccharomyces cerevisiae*. Appl Microbiol Biotechnol. 73**,** 1039-46.

Karhumaa, K., Garcia Sanchez, R., Hahn-Hagerdal, B., Gorwa-Grauslund, M. F., 2007b. Comparison of the xylose reductase-xylitol dehydrogenase and the xylose isomerase pathways for xylose fermentation by recombinant *Saccharomyces cerevisiae*. Microb Cell Fact. 6**,** 5.

Katahira, S., Ito, M., Takema, H., Fujita, Y., Tanino, T., Tanaka, T., Fukuda, H., Kondo, A., 2008. Improvement of ethanol productivity during xylose and glucose co-fermentation by xylose-assimilating *S. cerevisiae* via expression of glucose transporter Sut1. Enzyme Microb Technol. 43**,** 115-119.

Kim, S., Lee do, Y., Wohlgemuth, G., Park, H. S., Fiehn, O., Kim, K. H., 2013a. Evaluation and optimization of metabolome sample preparation methods for *Saccharomyces cerevisiae*. Anal Chem. 85**,** 2169-76.

Kim, S. R., Ha, S. J., Wei, N., Oh, E. J., Jin, Y. S., 2012. Simultaneous co-fermentation of mixed sugars: a promising strategy for producing cellulosic ethanol. Trends Biotechnol. 30**,** 274-82.

Kim, S. R., Park, Y. C., Jin, Y. S., Seo, J. H., 2013b. Strain engineering of *Saccharomyces cerevisiae* for enhanced xylose metabolism. Biotechnol Adv. 31**,** 851-61.

Kim, S. R., Skerker, J. M., Kang, W., Lesmana, A., Wei, N., Arkin, A. P., Jin, Y. S., 2013c. Rational and evolutionary engineering approaches uncover a small set of genetic changes efficient for rapid xylose fermentation in *Saccharomyces cerevisiae*. PLoS One. 8**,** e57048.

Kim, S. R., Xu, H., Lesmana, A., Kuzmanovic, U., Au, M., Florencia, C., Oh, E. J., Zhang, G., Kim, K. H., Jin, Y.-S., 2014. Deletion of *PHO13* encoding HAD type IIA phosphatase results in upregulation of the pentose phosphate pathway in yeast. Appl Environ Microbiol.

Kotter, P., Ciriacy, M., 1993. Xylose fermentation by *Saccharomyces cerevisiae*. Appl Microbiol Biotechnol. 38**,** 776-783.

Kuyper, M., Hartog, M. M., Toirkens, M. J., Almering, M. J., Winkler, A. A., van Dijken, J. P., Pronk, J. T., 2005a. Metabolic engineering of a xylose-isomerase-expressing *Saccharomyces cerevisiae* strain for rapid anaerobic xylose fermentation. Fems Yeast Res. 5**,** 399-409.

Kuyper, M., Toirkens, M. J., Diderich, J. A., Winkler, A. A., van Dijken, J. P., Pronk, J. T., 2005b. Evolutionary engineering of mixed-sugar utilization by a xylose-fermenting *Saccharomyces cerevisiae strain*. Fems Yeast Res. 5**,** 925-934.

Lamphier, M. S., Ptashne, M., 1992. Multiple Mechanisms Mediate Glucose Repression of the Yeast Gal1 Gene. Proc Natl Acad Sci U S A. 89**,** 5922-5926.

Latimer, L. N., Lee, M. E., Medina-Cleghorn, D., Kohnz, R. A., Nomura, D. K., Dueber, J. E., 2014. Employing a combinatorial expression approach to characterize xylose utilization in *Saccharomyces cerevisiae*. Metab Eng. 25**,** 20-9.

Lee do, Y., Fiehn, O., 2008. High quality metabolomic data for *Chlamydomonas reinhardtii*. Plant Methods. 4**,** 7.

Lee, S. H., Kim, S., Kwon, M. A., Jung, Y. H., Shin, Y. A., Kim, K. H., 2014a. Atmospheric vs. anaerobic processing of metabolome samples for the metabolite profiling of a strict anaerobic bacterium, *Clostridium acetobutylicum*. Biotechnol Bioeng. 111**,** 2528-36.

Lee, S. M., Jellison, T., Alper, H. S., 2014b. Systematic and evolutionary engineering of a xylose isomerase-based pathway in *Saccharomyces cerevisiae* for efficient conversion yields. Biotechnol Biofuels. 7.

Lee, W. J., Kim, M. D., Ryu, Y. W., Bisson, L. F., Seo, J. H., 2002. Kinetic studies on glucose and xylose transport in *Saccharomyces cerevisiae*. Appl Microbiol Biotechnol. 60**,** 186-191.

Li, C. K., Wen, A. Y., Shen, B. C., Lu, J., Huang, Y., Chang, Y. C., 2011. FastCloning: a highly simplified, purification-free, sequence- and ligation-independent PCR cloning method. BMC Biotechnol. 11.

Li, Y. C., Gou, Z. X., Liu, Z. S., Tang, Y. Q., Akamatsu, T., Kida, K., 2014. Synergistic effects of *TAL1* over-expression and *PHO13* deletion on the weak acid inhibition of xylose fermentation by industrial *Saccharomyces cerevisiae* strain. Biotechnol Lett. 36**,** 2011-21.

Liu, E. K., Hu, Y., 2010. Construction of a xylose-fermenting *Saccharomyces cerevisiae* strain by combined approaches of genetic engineering, chemical mutagenesis and evolutionary adaptation. Biochem Eng J. 48**,** 204-210.

Lu, C., Jeffries, T., 2007. Shuffling of promoters for multiple genes to optimize xylose fermentation in an engineered *Saccharomyces cerevisiae* strain. Appl Environ Microbiol. 73**,** 6072-7.

Lynd, L. R., Laser, M. S., Brandsby, D., Dale, B. E., Davison, B., Hamilton, R., Himmel, M., Keller, M., McMillan, J. D., Sheehan, J., Wyman, C. E., 2008. How biotech can transform biofuels. Nat Biotechnol. 26**,** 169-172.

Mans, R., van Rossum, H. M., Wijsman, M., Backx, A., Kuijpers, N. G., van den Broek, M., Daran-Lapujade, P., Pronk, J. T., van Maris, A. J., Daran, J. M., 2015. CRISPR/Cas9: a molecular Swiss army knife for simultaneous introduction of multiple genetic modifications in *Saccharomyces cerevisiae*. Fems Yeast Res. 15.

Matsushika, A., Goshima, T., Fujii, T., Inoue, H., Sawayama, S., Yano, S., 2012. Characterization of non-oxidative transaldolase and transketolase enzymes in the pentose phosphate pathway with regard to xylose utilization by recombinant *Saccharomyces cerevisiae*. Enzyme Microb Technol. 51**,** 16-25.

Matsushika, A., Inoue, H., Kodaki, T., Sawayama, S., 2009. Ethanol production from xylose in engineered *Saccharomyces cerevisiae* strains: current state and perspectives. Appl Microbiol Biotechnol. 84**,** 37-53.

Matsushika, A., Nagashima, A., Goshima, T., Hoshino, T., 2013. Fermentation of xylose causes inefficient metabolic state due to carbon/energy starvation and reduced glycolytic flux in recombinant industrial *Saccharomyces cerevisiae*. PLoS One. 8.

Ni, H., Laplaza, J. M., Jeffries, T. W., 2007. Transposon mutagenesis to improve the growth of recombinant *Saccharomyces cerevisiae* on D-xylose. Appl Environ Microbiol. 73**,** 2061-6.

Nijland, J. G., Shin, H. Y., de Jong, R. M., De Waal, P. P., Klaassen, P., Driessen, A. J. M., 2014. Engineering of an endogenous hexose transporter into a specific D-xylose

transporter facilitates glucose-xylose co-consumption in *Saccharomyces cerevisiae*. Biotechnol Biofuels. 7.

Olsson, L., Nielsen, J., 2000. The role of metabolic engineering in the improvement of *Saccharomyces cerevisiae*: utilization of industrial media. Enzyme Microb Technol. 26**,** 785-792.

Park, N. H., Yoshida, S., Takakashi, A., Kawabata, Y., Sun, H. J., Kusakabe, I., 2001. A new method for the preparation of crystalline L-arabinose from arabinoxylan by enzymatic hydrolysis and selective fermentation with yeast. Biotechnol Lett. 23**,** 411-416.

Park, S. J., Lee, S. Y., Cho, J., Kim, T. Y., Lee, J. W., Park, J. H., Han, M. J., 2005. Global physiological understanding and metabolic engineering of microorganisms based on omics studies. Appl Microbiol Biotechnol. 68**,** 567-579.

Peng, B. Y., Huang, S. C., Liu, T. T., Geng, A. L., 2015. Bacterial xylose isomerases from the mammal gut *Bacteroidetes* cluster function in *Saccharomyces cerevisiae* for effective xylose fermentation. Microb Cell Fact. 14.

Peng, B. Y., Shen, Y., Li, X. W., Chen, X., Hou, J., Bao, X. M., 2012. Improvement of xylose fermentation in respiratory-deficient xylose-fermenting *Saccharomyces cerevisiae*. Metab Eng. 14**,** 9-18.

Pereira, S. C., Maehara, L., Machado, C. M., Farinas, C. S., 2015. 2G ethanol from the whole sugarcane lignocellulosic biomass. Biotechnol Biofuels. 8**,** 44.

Reznicek, O., Facey, S. J., de Waal, P. P., Teunissen, A. W., de Bont, J. A., Nijland, J. G., Driessen, A. J., Hauer, B., 2015. Improved xylose uptake in *Saccharomyces cerevisiae* due to directed evolution of galactose permease Gal2 for sugar co-consumption. J Appl Microbiol.

Rizzi, M., Harwart, K., Buithanh, N. A., Dellweg, H., 1989. A kinetic study of the Nad+-xylitol-dehydrogenase from theyeast *Pichia-Stipitis* .6. J Ferment Bioeng. 67**,** 25-30.

Runquist, D., Hahn-Hagerdal, B., Bettiga, M., 2010. Increased ethanol productivity in xylose-utilizing *Saccharomyces cerevisiae* via a randomly mutagenized xylose reductase. Appl Environ Microbiol. 76**,** 7796-7802.

Ryan, O. W., Cate, J. H., 2014. Multiplex engineering of industrial yeast genomes using CRISPRm. Methods Enzymol. 546**,** 473-89.

Saeed, A. I., Bhagabati, N. K., Braisted, J. C., Liang, W., Sharov, V., Howe, E. A., Li, J., Thiagarajan, M., White, J. A., Quackenbush, J., 2006. TM4 microarray software suite. Methods Enzymol. 411**,** 134-93.

Sakihama, Y., Hasunuma, T., Kondo, A., 2015. Improved ethanol production from xylose in the presence of acetic acid by the overexpression of the *HAA1* gene in *Saccharomyces cerevisiae*. J Biosci Bioeng. 119**,** 297-302.

Sanchez, R. G., Karhumaa, K., Fonseca, C., Nogue, V. S., Almeida, J. R. M., Larsson, C. U., Bengtsson, O., Bettiga, M., Hahn-Hagerdal, B., Gorwa-Grauslund, M. F., 2010. Improved xylose and arabinose utilization by an industrial recombinant *Saccharomyces cerevisiae* strain using evolutionary engineering. Biotechnol Biofuels. 3.

Santangelo, G. M., 2006. Glucose signaling in *Saccharomyces cerevisiae*. Microbiol Mol Biol Rev. 70**,** 253-82.

Sedlak, M., Ho, N. W. Y., 2004. Characterization of the effectiveness of hexose transporters for transporting xylose during glucose and xylose co-fermentation by a recombinant *Saccharomyces* yeast. Yeast. 21**,** 671-684.

Senac, T., Hahn-Hagerdal, B., 1990. Intermediary metabolite concentrations in xylulose and glucose fermenting *Saccharomyces cerevisiae* cells. Appl Environ Microbiol. 56**,** 120-6.

Shao, Z. Y., Zhao, H., Zhao, H. M., 2009. DNA assembler, an in vivo genetic method for rapid construction of biochemical pathways. Nucleic Acids Res. 37.

Solis-Escalante, D., van den Broek, M., Kuijpers, N. G. A., Pronk, J. T., Boles, E., Daran, J. M., Daran-Lapujade, P., 2015. The genome sequence of the popular hexose-transport-deficient *Saccharomyces cerevisiae* strain EBY.VW4000 reveals LoxP/Cre-induced translocations and gene loss. Fems Yeast Res. 15.

Sonderegger, M., Sauer, U., 2003. Evolutionary engineering of *Saccharomyces cerevisiae* for anaerobic growth on xylose. Appl Environ Microbiol. 69**,** 1990-1998.

Stephanopoulos, G., 2007. Challenges in engineering microbes for biofuels production. Science. 315**,** 801-804.

Subtil, T., Boles, E., 2012. Competition between pentoses and glucose during uptake and catabolism in recombinant *Saccharomyces cerevisiae*. Biotechnol Biofuels. 5.

Takuma, S., Nakashima, N., Tantirungkij, M., Kinoshita, S., Okada, H., Seki, T., Yoshida, T., 1991. Isolation of xylose reductase gene of *Pichia stipitis* and its expression in *Saccharomyces cerevisiae*. Appl Biochem Biotech. 28-9**,** 327-340.

Taniguchi, M., Tohma, T., Itaya, T., Fujii, M., 1997. Ethanol production from a mixture of glucose and xylose by co-culture of *Pichia stipitis* and a respiratory-deficient mutant of *Saccharomyces cerevisiae*. J Ferment Bioeng. 83**,** 364-370.

Tantirungkij, M., Nakashima, N., Seki, T., Yoshida, T., 1993. Construction of xylose assimilating *Saccharomyces cerevisiae*. J Ferment Bioeng. 75**,** 83-88.

Tomitaka, M., Taguchi, H., Fukuda, K., Akamatsu, T., Kida, K., 2013. Isolation and characterization of a mutant recombinant *Saccharomyces cerevisiae* strain with high efficiency xylose utilization. J Biosci Bioeng. 116**,** 706-15.

Ulrich, E. L., Akutsu, H., Doreleijers, J. F., Harano, Y., Ioannidis, Y. E., Lin, J., Livny, M., Mading, S., Maziuk, D., Miller, Z., Nakatani, E., Schulte, C. F., Tolmie, D. E., Wenger, R. K., Yao, H. Y., Markley, J. L., 2008. BioMagResBank. Nucleic Acids Res. 36**,** D402-D408.

Van Vleet, J. H., Jeffries, T. W., Olsson, L., 2008. Deleting the para-nitrophenyl phosphatase (pNPPase), *PHO13*, in recombinant *Saccharomyces cerevisiae* improves growth and ethanol production on D-xylose. Metab Eng. 10**,** 360-369.

Vemuri, G. N., Aristidou, A. A., 2005. Metabolic engineering in the -omics era: Elucidating and modulating regulatory networks. Microbiol Mol Biol R. 69**,** 197-+.

Verduyn, C., Van Kleef, R., Frank, J., Schreuder, H., Van Dijken, J. P., Scheffers, W. A., 1985. Properties of the NAD(P)H-dependent xylose reductase from the xylose-fermenting yeast *Pichia stipitis*. Biochem J. 226**,** 669-77.

Verstrepen, K. J., Iserentant, D., Malcorps, P., Derdelinckx, G., Van Dijck, P., Winderickx, J., Pretorius, I. S., Thevelein, J. M., Delvaux, F. R., 2004. Glucose and sucrose: hazardous fast-food for industrial yeast? Trends Biotechnol. 22**,** 531-7.

Vilela Lde, F., de Araujo, V. P., Paredes Rde, S., Bon, E. P., Torres, F. A., Neves, B. C., Eleutherio, E. C., 2015. Enhanced xylose fermentation and ethanol production by engineered *Saccharomyces cerevisiae* strain. AMB Express. 5**,** 16.

Walfridsson, M., Hallborn, J., Penttila, M., Keranen, S., Hahn-Hagerdal, B., 1995. Xylose-metabolizing Saccharomyces cerevisiae strains overexpressing the *TKL1* and *TAL1* genes

encoding the pentose phosphate pathway enzymes transketolase and transaldolase. Appl Environ Microbiol. 61**,** 4184-90.

Wang, M., Yu, C., Zhao, H., 2015. Directed evolution of xylose specific transporters to facilitate glucose-xylose co-utilization. Biotechnol Bioeng.

Wisselink, H. W., Toirkens, M. J., Wu, Q., Pronk, J. T., van Maris, A. J. A., 2009. Novel evolutionary engineering approach for accelerated utilization of glucose, xylose, and arabinose mixtures by engineered *Saccharomyces cerevisiae* strains. Appl Environ Microbiol. 75**,** 907-914.

Young, E., Poucher, A., Comer, A., Bailey, A., Alper, H., 2011. Functional survey for heterologous sugar transport proteins, using *Saccharomyces cerevisiae* as a Host. Appl Environ Microbiol. 77**,** 3311-3319.

Young, E. M., Comer, A. D., Huang, H., Alper, H. S., 2012. A molecular transporter engineering approach to improving xylose catabolism in *Saccharomyces cerevisiae*. Metab Eng. 14**,** 401-11.

Young, E. M., Tong, A., Bui, H., Spofford, C., Alper, H. S., 2014. Rewiring yeast sugar transporter preference through modifying a conserved protein motif. Proc Natl Acad Sci U S A. 111**,** 131-136.

Zhang, G. C., Kong, II, Kim, H., Liu, J. J., Cate, J. H., Jin, Y. S., 2014. Construction of a quadruple auxotrophic mutant of an industrial polyploid *Saccharomyces cerevisiae* strain by using RNA-guided Cas9 nuclease. Appl Environ Microbiol. 80**,** 7694-701.

Zhou, H., Cheng, J. S., Wang, B. L., Fink, G. R., Stephanopoulos, G., 2012. Xylose isomerase overexpression along with engineering of the pentose phosphate pathway and

evolutionary engineering enable rapid xylose utilization and ethanol production by *Saccharomyces cerevisiae*. Metab Eng. 14**,** 611-622.